



Eidgenössische Technische Hochschule Zürich
Swiss Federal Institute of Technology Zurich



Master Thesis

Harnessing High-Altitude Floating Solar Power in Switzerland

Nicholas Eyring

Student Number: 09-815-572

September 30th, 2019

Supervisor: Dr. Noah Kittner

Group for Sustainability and Technology

Department of Management, Technology and Economics



Eidgenössische Technische Hochschule Zürich
Swiss Federal Institute of Technology Zurich

Declaration of originality

The signed declaration of originality is a component of every semester paper, Bachelor's thesis, Master's thesis and any other degree paper undertaken during the course of studies, including the respective electronic versions.

Lecturers may also require a declaration of originality for other written papers compiled for their courses.

I hereby confirm that I am the sole author of the written work here enclosed and that I have compiled it in my own words. Parts excepted are corrections of form and content by the supervisor.

Title of work (in block letters):

Harnessing High-Altitude Floating Solar Power In Switzerland

Authored by (in block letters):

For papers written by groups the names of all authors are required.

Name(s):

Eyring

First name(s):

Nicholas

With my signature I confirm that

- I have committed none of the forms of plagiarism described in the '[Citation etiquette](#)' information sheet.
- I have documented all methods, data and processes truthfully.
- I have not manipulated any data.
- I have mentioned all persons who were significant facilitators of the work.

I am aware that the work may be screened electronically for plagiarism.

Place, date

Zurich, 30.09.2019

Signature(s)

For papers written by groups the names of all authors are required. Their signatures collectively guarantee the entire content of the written paper.

Abstract

Switzerland's mandate to phase-out nuclear power has prompted the need for a large-scale increase in domestic renewable electricity production. Recent findings have demonstrated the potential for Swiss solar power to play a dominant role in this capacity expansion, with high-altitude solar installations being particularly effective in adding clean energy while alleviating the temporal mismatch between electricity supply and demand (Kahl et al., 2019). However, given the limited availability of land in Switzerland, it is difficult to find suitable locations for harnessing solar power on a large scale. Floating solar is an emerging technology which can substantially increase solar output where land is limited. To take advantage of the benefits of high-altitude solar while addressing the need for utility-scale space, this thesis investigates the potential contribution of floating solar power on alpine water bodies to help bridge the gap left in the wake of nuclear withdrawal. Taking a bottom-up approach, we quantify the technical and economic potential of 82 prospective high-altitude sites using high-resolution meteorological and market data. Our results show substantial technical potential, emission reductions, and incentives for Swiss hydropower utilities to integrate with floating solar technologies at high-altitude. However, significant cost reductions are needed for economic viability without subsidies or storage, indicating the need for further engineering. As the floating solar industry matures, high-altitude floating solar technology on Swiss hydro reservoirs is set to become an attractive option for capacity expansion.

Acknowledgments

First, I would like to thank Dr. Noah Kittner for his guidance and valuable feedback throughout the project. Our regular discussion sessions were great sources of inspiration and direction. In addition, I would like to thank Dominik Neumayr for his input and for originally stimulating my interest in building solar power systems on Swiss hydro reservoirs. I would also like to thank my fellow master students and the SusTec team for the friendly working environment and keen participation in discussions. Finally, I am eternally grateful to my friends and family for their everlasting support.

Table of Contents

Abstract.....	V
Acknowledgments	VII
List of Abbreviations	X
List of Symbols.....	XI
1 Introduction	1
2 Research Questions	4
2.1 Contribution to Literature	5
3 Data & Methodology.....	6
3.1 Overview of Data Sets and Sources	6
3.2 Implementation – HASPR Research Environment	8
3.3 Water Body Selection & Attributes	9
3.4 Generation Profiles.....	11
3.4.1 Modelling Historic Generation Profiles.....	12
3.4.2 Calculating Expected Generation Profiles	15
3.4.3 Aggregation of Individual Generation Profiles.....	16
3.5 Supply/Demand Mismatch.....	17
3.6 CO2 Offset	17
3.7 Revenue Analysis.....	18
3.8 Costs Analysis.....	18
3.9 Investment Profiles.....	20
4 Results	22
4.1 Technical Potential.....	23
4.1.2 Addressing the Swiss Temporal Supply/Demand Mismatch.....	28
4.1.3 CO2 Offset Analysis	29
4.2 Economic Potential	30
4.2.1 Cost Targets	33
5 Discussion & Implications.....	34
5.2 Limitations & Further Research	37
6 Conclusion & Outlook.....	38
A Appendix	39
A1 Complete List of HASPR Scripts & Documentation	39
A2 Full Water Body Sample and Collected Attributes	41
A3 Exchange Rates	42
A4 Tables of Results by Scenario	42
References.....	47

List of Abbreviations

CMSAF	EUMETSAT Satellite Application Facility on Climate Monitoring
CO2	carbon dioxide
EMPA	Swiss Federal Laboratories for Materials Science and Technology
ENTSO-E	European Network of Transmission System Operators for Electricity
HASPR	High-Altitude Solar Power Research python library
LCOE	Levelized Cost of Electricity
NAN	Not A Number
NPV	Net Present Value
O&M	Operations and Maintenance
POA	Plane of Array
SID	Surface Incoming Direct irradiance for one horizontal square meter
SIDIFF	Surface Incoming Diffuse irradiance for one horizontal square meter
SIS	Surface Incoming Shortwave irradiance for one horizontal square meter
swisstopo	Swiss Federal Office of Topography swisstopo

List of Symbols

AO	annual operations cost
α	angle between solar direct beam and panel normal vector
B_i	bid revenue for site i over one year
β	panel tilt
CC	capital costs
CF_n	cash flow in year n
DR	discount rate
E_{POA}	incoming solar energy received by a panel in a POA model
E_{direct}	energy of direct component projected onto panel normal vector
$E_{diffuse}$	energy of diffuse component projected onto panel normal vector
$E_{ground-reflected}$	energy of ground-reflected component projected onto panel normal vector
E_{out}	electrical energy output
η	system efficiency
$g_{i,T=t}$	historical generation per square meter of site i at time step t
$\hat{g}_{i,T=t}$	expected generation per square meter for site i at time step t
$G_{T=t}$	electrical energy generation across the entire sample at time step t
IP	initial production
L	system lifetime in years
$OM\%$	operations and maintenance cost as percentage of capital costs
PAZ	panel azimuth
$price_t$	day-ahead slot price at time t
PSA_i	panel surface area at site i
RV	residual value
$\rho_{surface}$	surface albedo
SAZ	solar azimuth
SDR	system degradation rate
SID	surface incoming direct irradiance for one horizontal square meter
$SIDIFF$	surface incoming diffuse irradiance for one horizontal square meter

SIS	surface incoming shortwave irradiance for one horizontal square meter
SZA	solar zenith angle
$\sigma_{i,T=t}^2$	variance in historic output per square meter of site i at time step t

1 Introduction

The devastating effects of climate change have resulted in an increasing global urgency to abate carbon dioxide (CO₂) emissions (Hansen et al., 2016). As a response to the pressing environmental impact of the energy sector, Switzerland has adopted the *Energy Strategy 2050* policy to transition to a clean, net-zero emissions energy system by 2050 (Bundesamt für Energie BFE, 2018a). The strategy includes a gradual phase-out of nuclear power. Switzerland's five nuclear power plants generated 24.4 TWh in 2018, accounting for over a third of the country's electricity production (Bundesamt für Energie BFE, 2019). The new policy aims to bridge the gap left in the wake of nuclear withdrawal through the development of Swiss renewable sources, resulting in a capacity expansion problem as depicted in Figure 1.

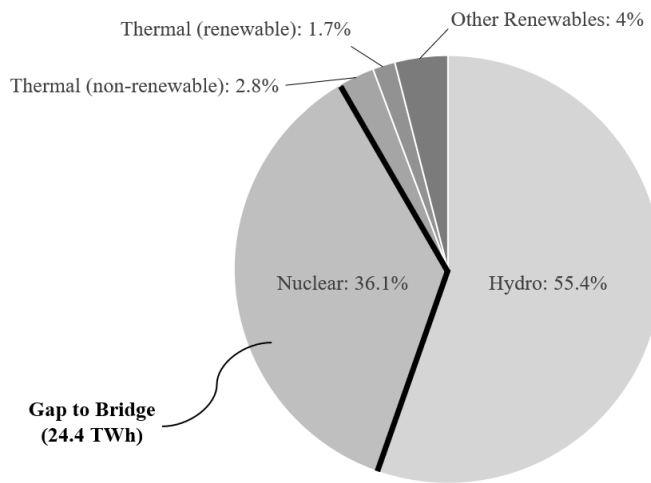


Figure 1: Breakdown of Swiss electricity production in 2018 with an illustration of nuclear capacity to substitute with renewable sources. Values are taken from (Bundesamt für Energie BFE, 2019).

Consistently providing renewable electricity to satisfy varying demand is difficult (Davis et al., 2018) and Switzerland already faces a significant temporal mismatch between demand and supply with a large winter deficit (Figure 2). Current research indicates that Swiss electricity demand can fully be addressed by substituting nuclear output with a solar-dominated renewable portfolio; however, planning and land access have been identified as key barriers to the required large-scale increase in solar capacity (Bartlett et al., 2018). Furthermore, Swiss solar power production is typically high in summer when demand is low and insufficient in winter when

electricity is most needed, with recent findings showing that mountain installations combined with higher tilt angles are suitable for rectifying this mismatch (Kahl et al., 2019).

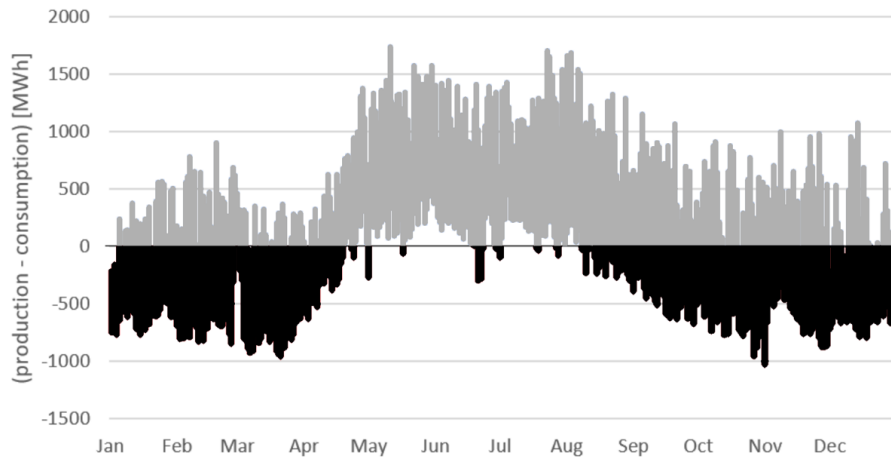


Figure 2: Swiss mismatch between electricity supply and demand in 2018 (15-minute resolution) with black data points representing insufficient domestic supply. Values are taken from (Swissgrid, 2019).

High-altitude solar sites generally profit from greater production potential due to lower radiation extinction and the high reflectance of snow (Blumthaler, 2012). Solar panel efficiency also increases considerably at low temperatures (Chitturi et al., 2018), providing further motivation for the development of high-altitude arrays. Given the need for utility-scale space, the use of water bodies is an interesting alternative to building traditional ground-mounted solar installations in mountainous terrain. In addition, the large number of hydropower facilities in the Swiss alps could provide water bodies with grid connections and possibilities for integration – a key element of net-zero emissions energy systems (Davis et al., 2018). However, the potential for such systems has not been quantified or incorporated into any currently published studies on the Swiss electricity mix. To address this literature gap, our study explores the use of emerging floating solar technology on Swiss high-altitude water bodies as a viable way to substantially increase domestic renewable electricity production.

Floating solar technology allows for new opportunities to increase solar capacity, especially in countries with high opportunity costs of land use (World Bank Group et al., 2018). This observation provides a key motive for our examination of the technology's implementation in Switzerland to circumvent the barrier of land access. In addition, floating solar technology

boasts multiple benefits compared to ground installations, including increased system efficiency due to the natural cooling effect of water (Campana et al., 2019). Floating arrays also diminish the need for major land preparation and allow for highly modular and reversible systems, implying less environmental impact than ground-mounted installations (Cazzaniga et al., 2019). Moreover, the use of floating arrays spares precious water resources by significantly reducing evaporation rates (Ranjbaran et al., 2019). Costs for floating arrays are currently slightly higher than ground-mounted panels but are expected to decrease as production processes mature (World Bank Group et al., 2018). As an emerging technology, the global installed capacity of floating solar has rapidly grown since 2012 (Figure 3), expanding from 5 MWp in 2013 to 1.1 GWp in September 2018 (World Bank Group et al., 2018). Robust floating systems which are capable of dealing with variable depths and harsh conditions have recently become available as standard products (Ciel & Terre International, 2019), suggesting that the time is right to examine the use of floating solar technology at high-altitude sites in Switzerland.

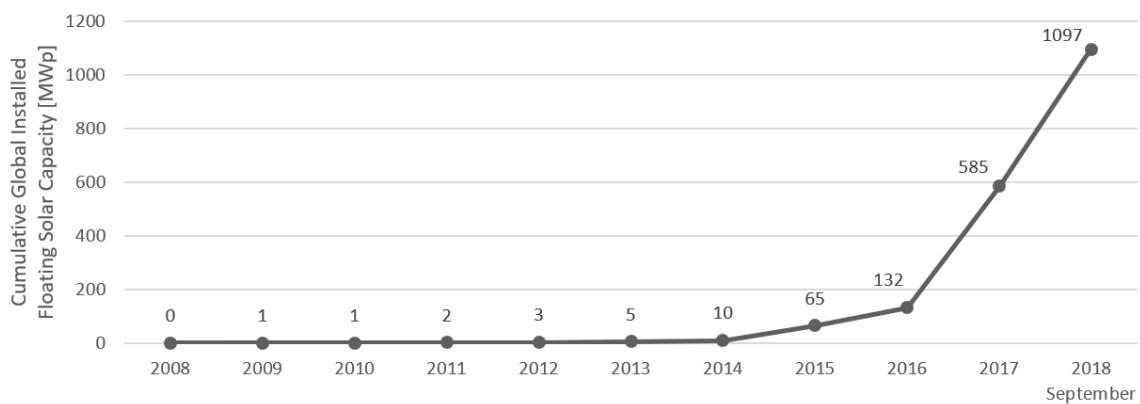


Figure 3: Yearly development of cumulative global installed floating solar capacity. Values are taken from (World Bank Group et al., 2018).

To shed light on the technical and economic potential of Swiss high-altitude floating solar power, we take a bottom-up approach by calculating high-resolution generation profiles for a practical sample of water bodies. Historic high-resolution meteorological data was used to implement this calculation. As a result, we find that large-scale high-altitude floating solar power can significantly contribute to solving Switzerland's capacity expansion problem.

2 Research Questions

This thesis aims to investigate the use of high-altitude floating solar energy to alleviate the problems Switzerland is facing in its electricity mix. To achieve this, we address the following two primary research questions:

1. *What is the technical potential of high-altitude floating solar power in Switzerland?*
2. *To what extent can the temporal mismatch between Swiss power supply and demand be addressed with high-altitude floating solar arrays?*

The purpose of the first research question is to determine how much and when energy can be harnessed through the installation of high-altitude floating solar systems in Switzerland. We present maximum values given the amount of incoming solar energy and available surface area of a feasible sample of high-altitude water bodies as well as conservative estimates of real-world production and impact under multiple design configurations.

Our second research question intends to determine the market potential of high-altitude floating solar power in Switzerland. Temporal mismatches between production and consumption pose a significant problem with integrating solar (and other renewables) into the Swiss electricity mix (Bartlett et al., 2018). It is therefore critical to analyze how the energy produced by floating solar can be incorporated given Swiss electricity production and consumption patterns, if it is economically viable to do so, and the potential impact on Switzerland's temporal market mismatch.

By addressing these two research questions, this thesis aims to determine how high-altitude floating solar can effectively contribute to the Swiss electricity mix – thereby providing insight for both the Swiss government and industry who would be interested to know if floating solar is a technology worth pursuing and how it could be added to the arsenal of tools available to reach Switzerland's energy targets.

2.1 Contribution to Literature

This study intends to contribute to current literature in two ways: first by expanding on the few published papers on the topic of floating solar through the presentation of an analytical framework for quantifying the capabilities of the technology at a high temporal resolution with Switzerland as the country of interest (research question 1), and second by building on recent results showing considerable potential of solar installations in the Swiss alps (Kahl et al., 2019). These results are based on a top-down analysis which does not consider water bodies. We therefore build on these insights by taking a realistic bottom-up approach to determine the extent to which Swiss high-altitude water bodies can address the seasonal mismatch and relieve pressure on Switzerland's energy sector using floating solar technology (research question 2).

3 Data & Methodology

To address our two primary research questions through a bottom-up approach, we first need to determine the output of potential floating solar installations over time given a sample of water bodies. Solar power is intermittent by nature and can vary significantly even over short periods of time – not only due to day/night cycles, but also due to varying meteorological conditions such as cloud cover and the presence of snow (Kahl et al., 2019). National electricity production and consumption also fluctuate greatly over the course of any given day (Swissgrid, 2019). This being the case, it is desirable to obtain output profiles with a high temporal resolution to analyze the contribution of potential solar sites to the electricity mix. We therefore use a model based on high-resolution meteorological data to determine the electricity generated by prospective floating solar power systems. By combining water body data with historic meteorological data, we obtain historic generation profiles in 30-minute resolution for conceivable floating solar sites which subsequently serve as input for further analyses. An overview of our approach is presented in Figure 4 below:

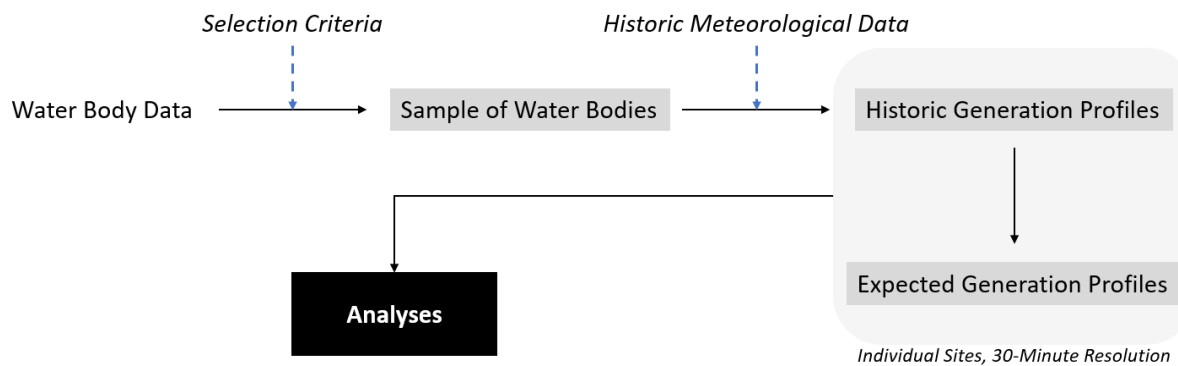


Figure 4: Overview of our methodology based on generation profiles of individual sites.

3.1 Overview of Data Sets and Sources

A summary of the data sets used in our analysis can be found in Table 1. Detailed descriptions of the variables, why they were selected, and their use can be found in the subsections dedicated to the corresponding steps in our analysis.

To establish our sample of potential floating solar sites, Swiss water body data was sourced directly from the *Swiss Federal Office of Topography swisstopo* (swisstopo) via their interactive map of official survey and geological data sets (Federal Office of Topography swisstopo, 2019) while the associated Swiss hydropower plant data was retrieved from the yearly hydro statistics report published by the *Swiss Federal Office of Energy* (Bundesamt für Energie BFE, 2018b). To calculate historic generation profiles, solar position was computed via Pysolar – a python implementation of the Solar Position Algorithm (Pysolar Development Team, 2019) – with the rest of our high-resolution climate data being provided by the *EUMETSAT Satellite Application Facility on Climate Monitoring* (CMSAF) (Karlsson et al., 2017) (Pfeifroth et al., 2019). To analyze the Swiss electricity supply/demand mismatch, high-resolution data on total Swiss electricity consumption and production was retrieved from *Swissgrid*, the Swiss transmission system operator (Swissgrid, 2019). For our revenue analysis, Swiss electricity price data was sourced from the *European Network of Transmission System Operators for Electricity* (ENTSO-E) (ENTSO-E Transparency Platform, 2019). Finally, Swiss grid carbon intensity data for our CO₂-offset analysis was retrieved from an *ETH Zürich* study distributed by the *Swiss Federal Laboratories for Materials Science and Technology* (EMPA) (Chevrier, Smith, & Bollinger, 2016).

Value	Time Period	Temporal Resolution	Spatial Resolution	Data Source
<i>Water Bodies</i>				
Coordinates	-	-	-	(Federal Office of Topography swisstopo, 2019)
Altitude	-	-	-	(Federal Office of Topography swisstopo, 2019)
Surface area	-	-	-	(Federal Office of Topography swisstopo, 2019)
Dams under Swiss federal supervision	3 July 2018	-	-	(Federal Office of Topography swisstopo, 2019)
<i>Hydro Installations</i>				
Coordinates	1 January 2018	-	-	(Bundesamt für Energie BFE, 2018)
Associated water bodies	1 January 2018	-	-	(Bundesamt für Energie BFE, 2018)
Plant type	1 January 2018	-	-	(Bundesamt für Energie BFE, 2018)
<i>Meteorological Data</i>				
Surface incoming shortwave irradiance	2008 - 2017	30 minutes	0.05 x 0.05 deg	CMSAF (Pfeifroth et al., 2019)
Surface incoming direct irradiance	2008 - 2017	30 minutes	0.05 x 0.05 deg	CMSAF (Pfeifroth et al., 2019)
Surface albedo	2006 - 2015	5 days	0.25 x 0.25 deg	CMSAF (Karlsson et al., 2017)
Solar position (altitude, azimuth)	-	-	-	(Pysolar Development Team, 2019)
<i>Electricity Market</i>				
Total Swiss electricity consumption	2018	15 minutes	-	(Swissgrid, 2019)
Total Swiss electricity production	2018	15 minutes	-	(Swissgrid, 2019)
Swiss day-ahead electricity prices	2015 - 2018	1 hour	-	(ENTSO-E Transparency Platform, 2019)
Grid carbon intensity (CO ₂ -equivalent)	2015	1 hour	-	(Chevrier et al., 2016)

Table 1: Summary of data sets and sources.

3.2 Implementation – HASPR Research Environment

To conduct a thorough bottom-up study of potential solar sites, the High-Altitude Solar Power Research python library (HASPR) was written from scratch. HASPR grants users the ability to model the output of solar arrays given high-resolution meteorological data. For the benefit of solar energy researchers, the library is open-source under the MIT license and can be found on GitHub at <https://github.com/bonesbb/HASPR>. Python was chosen due to its popularity in the scientific and data analytics communities and its strength as a scripting language. The HASPR library consists of the following key object classes to facilitate scripted data-driven solar energy research:

- *Dataset* class: facilitates dealing with data sets in a standardized way.
- *Model* class: used to define models which interact with *Dataset* objects in a standardized way.
- *Result* class: a one-size-fits-all way for *Model* objects to write their output to the local disk.

The python environment we created allows any researcher to pick up where we left off with ease to gain concrete high-resolution insights on solar energy, including batch computing capabilities for very large models.

HASPR consists of a collection of scripts separated into folders depending on their type of use. The *Generation Scripts* folder contains scripts which calculate output profiles of potential solar sites under various panel positions in 30-minute resolution. *Processing Scripts* contains scripts which are used to convert 30-minute results into lower resolutions as well as scripts to remove leap days for consistency. The *Analysis Scripts* folder comprises scripts which run analyses on generation profiles given various additional data sets. At the core of HASPR lies the *haspr.py* script which can be found in the root folder. This file serves as a background script containing common functions and class definitions which are used by all other HASPR scripts. A complete list of all HASPR files and their use can be found in Appendix A1.

The HASPR environment is designed to accept data sets in NetCDF4 format (common for meteorological data) or CSV format and outputs *Result* objects as CSV files. An overview of the HASPR system and data flows is depicted in Figure 5. Appendix A1 presents further information on HASPR’s use and the specific implementation of its functions and models.

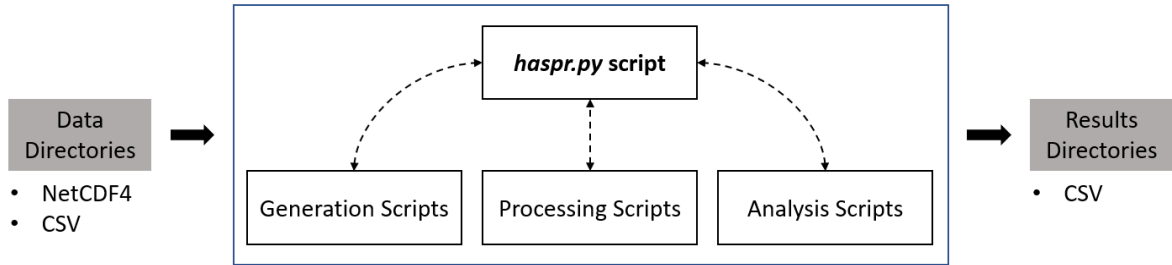


Figure 5: Overview of HASPR research environment and data flows.

3.3 Water Body Selection & Attributes

Building industrial-scale power facilities in the mountains can be very expensive and difficult. To obtain a conservative lower bound for the potential of utility-scale high-altitude floating solar power in Switzerland, we focus on lakes with existing road access and nearby power infrastructure. This implies significantly lower construction costs, especially if the system’s output can be connected to the low-voltage side of existing grid-scale transformers, thereby eliminating the need to construct utility-grade transformers and surge-protection systems. Due to the intermittency of solar power, coupling floating solar sites with a storage system such as pumped hydro is crucial (Ranjbaran et al., 2019). Given the large number of dams and storage hydro plants in the Swiss mountains, we selected sites associated with existing hydropower installations to obtain a sample of water bodies with the characteristics outlined above. We define high-altitude as anything higher than 1000 meters above sea level and our sample encompasses all dammed water bodies in Switzerland above this threshold which are associated with storage or pumped-storage hydro facilities. Only dammed water bodies are considered since it is likely that disturbing pristine natural lakes would face heavier barriers to construction than building on artificial water bodies. As a result of these filters, our sample allows us to obtain a realistic lower bound to conservatively answer our research questions.

The criteria for adding a water body to our list of potential high-altitude floating solar sites is presented in Figure 6. The Swiss hydro statistics data set we use provides us with a list of all hydro installations with a capacity above 300 kW – complete with coordinates, plant types, and associated water bodies (Bundesamt für Energie BFE, 2018b). Systematically processing each data point in the hydro statistics data set, the associated water bodies were added to our list of potential sites if all five criteria were met.

- Criterion 1:** Water body is entirely in Switzerland
- Criterion 2:** Water body is associated with a storage or pumped-storage hydro facility
- Criterion 3:** Water body altitude is greater than 1000 m
- Criterion 4:** Surface area of water body is greater than 1000 m²
- Criterion 5:** Water body is dammed

Figure 6: List of criteria for adding water bodies to our sample.

Criterion 2 was automatically fulfilled given our search method. Once a water body associated with a storage or pumped-storage hydro facility had been identified, criterion 1 and criterion 3 were tested by reading directly from swisstopo's interactive map (Federal Office of Topography swisstopo, 2019). Surface area data was acquired by using the map's *VECTOR25 Primary surfaces* overlay while the location of dams was determined by overlaying the *dams under federal supervision* data set. Site coordinates were collected by right-clicking roughly in the geometric center of the water body to display point information. A rough estimate of the lake's center suffices as our meteorological data sets are pixelated with a spatial resolution of roughly 5 km.

An integer ID was assigned to each individual water body to easily keep track of locations. A database of potential sites (water bodies) was then established and populated in spreadsheet form, containing all collected water body attributes. From this spreadsheet, tailored CSV files were extracted to serve as model inputs for HASPR scripts.

The described selection process results in a sample of 82 potential sites for high-altitude floating solar power production in Switzerland. A summary of our sample is presented in Table 2 while a full breakdown including site IDs, names, coordinates, altitudes, surface areas, associated hydro facilities, and further attributes can be found in Appendix A2.

Number of Water Bodies	Total Surface Area (km²)	Average Surface Area (km²)	Average Altitude (m)
82	50.1	0.61	1783

Table 2: Summary of the sample of water bodies used for our analysis.

3.4 Generation Profiles

A generation profile expresses the electricity output over time of a potential floating solar site. The primary factor in determining the output of a solar power system is the level of incoming solar radiation (Antonanzas et al., 2016). Consequently, our approach calculates expected generation profiles for each site in our sample based on the most recent 10 years of available historic radiation data. Climate data records provided by CMSAF were used due to their high temporal resolution (30 minutes for radiation data) as well as their extensive validation and calibration, as described in (Pfeifroth et al., 2019).

Panel position has a significant influence on the power generated by floating solar arrays (Cazzaniga et al., 2018). Similar to ground-mounted solar plants, floating solar systems exist in a variety of design configurations ranging from fixed-position systems to solar tracking designs (Ranjbaran et al., 2019). To present and compare results for multiple system types, we calculate generation profiles for each of the five panel position cases listed in Table 3.

Panel Configuration	Description
Case 1: Flat panels	Panels placed horizontally on surface
Case 2: Tracking panels	Panel normal vector is aligned with solar position at all times
Case 3: Fixed panels with 12-degree tilt, optimized for total production	Total output optimization of standard product from current floating solar market leader (Ciel & Terre International, 2019)
Case 4: Fixed panels with 12-degree tilt, optimized for winter production	Winter output optimization of standard product from current floating solar market leader (Ciel & Terre International, 2019)
Case 5: Fixed panels with tilt between 30 and 65 degrees, optimized for winter production	Configuration to maximize winter production with high-altitude fixed panels (Kahl et al., 2019)

Table 3: Outline of investigated floating solar design configurations.

3.4.1 Modelling Historic Generation Profiles

Solar energy harnessed by a panel can be broken down into three components: the energy from the direct beam (direct component), the energy from all the scattered beams in the sky (diffuse component), and finally the beams reflected from the ground (ground-reflected component) (Kahl et al., 2019). For simplicity, we assume that the diffuse radiation is isotropic, meaning that the scattered beams are evenly distributed over the hemisphere in question. Isotropic Plane of Array (POA) models are suitable for determining baseline energy production – calculating panel output by projecting multiple incoming components onto a vector which is perpendicular to the panel’s surface (Lave et al., 2015). Multiplying the resulting incoming solar energy per square meter by the system’s efficiency yields the amount of electricity generated per unit of surface area. This process is described in Equations (1) and (2), where η represents system efficiency.

$$E_{POA} = E_{direct} + E_{diffuse} + E_{ground-reflected} \quad (1)$$

$$E_{out} = \eta \cdot E_{POA} \quad (2)$$

The first term in Equation (1) denotes the projection of the direct beam onto the panel normal vector. We define α as the angle between these two vectors, SZA as the solar zenith angle and use the Surface Incoming Direct irradiance for one horizontal square meter (SID) to rewrite the direct component as shown in Equation (3). The cosine of α can be determined by transforming the current solar position and panel attitude from two points in spherical coordinates to two

vectors in cartesian space. Since we are only interested in the angle, assuming both vectors have an amplitude of 1 allows us to determine the cosine of α via their scalar product. The result is presented in Equation (4), where SAZ represents solar azimuth, β is the panel tilt, and PAZ denotes panel azimuth. If the sun is behind the panel ($\cos(\alpha) < 0$), we set E_{direct} to zero.

$$E_{direct} = \frac{SID}{\cos(SZA)} \cdot \cos(\alpha) \quad (3)$$

$$\begin{aligned} \cos(\alpha) = & \sin(SZA) \cdot \cos(SAZ) \cdot \sin(\beta) \cdot \cos(PAZ) \\ & + \sin(SZA) \cdot \sin(SAZ) \cdot \sin(\beta) \cdot \sin(PAZ) \quad (4) \\ & + \cos(SZA) \cdot \cos(\beta) \end{aligned}$$

The second term in Equation (1) represents the projection of all scattered beams onto the panel normal vector. To express this term assuming isotropic diffuse radiation, we multiply the Surface Incoming Diffuse irradiance for one horizontal square meter (SIDIFF) by a sky view factor as described in (Hay, 1993). Equation (5) presents the result.

$$E_{diffuse} = SIDIFF \cdot \left(\frac{1+\cos(\beta)}{2} \right) \quad (5)$$

The energy from beams reflected off the ground and nearby surfaces is represented by the third and final term in Equation (1). We assume that the reflection is isotropic, allowing us to use a ground view factor combined with the surface albedo ($\rho_{surface}$) and Surface Incoming Shortwave irradiance for one horizontal square meter (SIS) as presented in (Hay, 1993). The resulting expression for the ground-reflected component is shown in Equation (6).

$$E_{ground-reflected} = SIS \cdot \rho_{surface} \cdot \left(\frac{1-\cos(\beta)}{2} \right) \quad (6)$$

Although three radiation data sets are mentioned in our model's equations, only two are necessary to collect since SIS is defined as the sum of SID and SIDIFF (Pfeifroth et al., 2019).

SIS and SID data sets were retrieved at a temporal resolution of 30 minutes for the years 2008-2017. However, the maximum resolution provided by CMSAF for surface albedo is 5 days with values only until the end of the year 2015. To obtain historic generation profiles in 30-minute resolution, we take the average of the 5-day surface albedo over the years 2006-2015 at the coordinates in question. Solar altitude and azimuth are calculated for every time step via Pysolar (with $SZA = 90 - \text{solar altitude}$) and panel position parameters were set for each case in Table 3 as outlined below:

Case 1: Flat panels

- $\beta = 0$, implying that $E_{POA} = SIS$

Case 2: Tracking panels

- At every time step, $\beta = SZA$ and $PAZ = SAZ$

Cases 3 & 4: Fixed panels with 12-degree tilt

These cases represent the standard configuration of the current floating solar market leader (Ciel & Terre International, 2019). Brute-force with an increment of 10 degrees was used to optimize PAZ with $\beta = 12$ for both winter production (November-April, Case 3) and total production (Case 4) for the year 2017, representing the most recent radiation data we have.

Case 5: Fixed panels with tilt between 30 and 65 degrees, optimized for winter

The configuration needed to maximize winter production with high-altitude fixed panels in Switzerland entails setting the tilt between 30 and 65 degrees (Kahl et al., 2019). For this case, we used brute-force to optimize PAZ (increment = 10 degrees) and optimized β between 30 and 65 degrees (increment = 5 degrees). The optimization was run for the year 2017, maximizing winter output (November-April).

Historic generation profiles were calculated for every water body in our sample, for all five panel position cases, and for all 10 years between 01.01.2008 and 31.12.2017. As a baseline, system efficiency was set to 15%, as applied in (Kahl et al., 2019).

Note on execution time and hardware used:

Using brute-force to optimize fixed-tilt positions in Cases 3, 4, and 5 requires us to compute a very large number of historic generation profiles. Our implementation of all models described herein can run to scale with as little as 1 GB of RAM. However, the bottleneck lies in the CPU. Typical execution time for a model thread can be up to 15 minutes per generation profile per year on a modern processor. To speed things up, we executed in parallel batches on the Euler cluster at ETH Zürich. Respecting the usage limits of Euler for non-shareholders, acceleration was achieved by slicing our models into 30 standard batch jobs at a time, each calculating 20 generation profiles and running in 4-hour parallel slots. This framework implies a maximum capacity of 600 yearly 30-minute resolution generation profiles computed every 4 hours. A total of 1604 batch jobs were executed on Euler, amounting to approximately 250 days of processor time.

Note on missing data values:

Our meteorological satellite data was obtained through highly-sensitive geostationary instruments with a non-zero probability of downtime. This results in multiple Not A Number (NAN) data points. The number of NAN values in the retrieved data differs from year to year and depends on the coordinates of the site in question. Our SIS and SID values are calibrated and validated by CMSAF. However, NANs persist in the data sets. To take the inconsistency of the satellite data into account, HASPR includes the total number of NANs in each generation profile's output and conservatively sets all NANs to zero.

3.4.2 Calculating Expected Generation Profiles

Given 10 years of historic generation output, we calculate the expected yearly generation profile per square meter for each site by averaging the historic values at every time step according to Equation (7), where $\hat{g}_{i,T=t}$ is the expected generation per square meter for site i at time step t and $g_{i,T=t}$ is the corresponding historic generation per square meter. For consistency, leap days are disregarded.

Due to the intermittent nature of solar power, it is desirable to obtain insights on the variability and uncertainty of electricity production. For our analysis, we determine a lower bound for 30-minute site output at 95% confidence by adding a noise term to Equation (7). To achieve this, output is modelled as the expected value of a stochastic variable following a normal distribution centered around the average historic production and with a variance equal to the variance in historic generation for the corresponding time step as expressed in Equation (8), where $\sigma_{i,T=t}^2$ is the variance in historic output per square meter of site i at time step t . The noise term is used solely to determine lower bounds as its use to determine expected output could falsely add power from the tails of the distribution. Equation (8) is consistent with Equation (7) as the expected value of the normal distribution simply equals its mean.

$$\hat{g}_{i,T=t} = \text{average}(g_{i,T=t}) \quad (7)$$

$$\hat{g}_{i,T=t} = E[n_{i,T=t}], \text{ where } n_{i,T=t} \sim N(\text{average}(g_{i,T=t}), \sigma_{i,T=t}^2) \quad (8)$$

Our HASPR implementation of these calculations produces yearly expected generation profiles in 30-minute resolution along with the lower bound (95% confidence), the variance, and the normalized variance (equal to variance divided by expected output) at each time step.

3.4.3 Aggregation of Individual Generation Profiles

Historic and expected generation profiles compute the electricity generated at individual sites in terms of energy per square meter. Multiplying by the respective panel surface area results in the actual energy produced. To gain insight on the potential electricity production of our entire water body sample, we take the sum of the expected energy generation across all sites. This calculation is expressed in Equation (9), where $G_{T=t}$ denotes the electrical energy generation across the entire sample at time step t and PSA_i is the panel surface area at site i . To obtain a range of results, PSA_i was set to various percentages of the corresponding water body's surface area.

$$G_{T=t} = \sum_i (\hat{g}_{i,T=t} \cdot PSA_i) \quad (9)$$

3.5 Supply/Demand Mismatch

We measure the Swiss electricity supply/demand mismatch at a given point in time by taking the difference between total electrical energy production and total electrical energy consumption in the Swiss control block. If consumption is greater than production, the difference needs to be imported from neighboring countries. To quantify the extent to which floating solar power can address the Swiss domestic supply/demand mismatch, we determine the amount of these imports which could be offset given aggregate expected generation profiles for each of the cases listed in Table 3.

The data needed for this analysis is available in 15-minute resolution from (Swissgrid, 2019), allowing us to compare the mismatch with aggregated generation profiles in 30-minute resolution by summing the difference between production and consumption in half-hour steps. 2018 data is used to represent the most recent values available for an entire year.

3.6 CO2 Offset

To gain insight on the positive environmental effects of installing high-altitude floating solar power in Switzerland, we estimate the amount of CO2-equivalent greenhouse gas emissions which could be offset for various aggregate generation profiles. Given the hourly intensity of CO2-equivalent emissions for the Swiss electrical grid from (Chevrier et al., 2016), we multiply the emission values per unit of energy by the hourly floating solar output to obtain the CO2-equivalent offset if floating solar power is used as a substitute for current non-zero emissions energy sources – assuming the power is sold at the time of generation. To put the results into perspective, we compare the offset with annual European CO2 emissions from coal power with data provided by (U.S. Energy Information Administration, 2019).

3.7 Revenue Analysis

Our bottom-up analysis of the market potential of floating solar in Switzerland requires us to compute the potential revenue of each site in our sample. To determine the revenue potential without government intervention, subsidies and feed-in tariffs are not considered. Instead, we calculate the corresponding revenue profile for a given generation profile by assuming that power is sold at the time of production on the Swiss wholesale day-ahead market, for which hourly prices are provided for the years 2015-2018 by (ENTSO-E Transparency Platform, 2019). To sell power on this market, bids must be defined for hourly slots in increments of 0.1 MWh (Abrell, 2017). We therefore round the generation over a given slot down to the nearest 0.1 MWh to determine bid revenue. Equation (10) expresses the revenue calculation for one site, where B_i represents the bid revenue for site i over the year in question and $price_t$ denotes the slot price at time t . Values for expected revenue were calculated by averaging the results over the period 2015-2018.

$$B_i = \sum_{t \in year} (\text{round_down}(\sum_{u \in [t, t+1h]} \hat{g}_{i,T=u} \cdot PSA_i, 0.1MWh) \cdot price_t) \quad (10)$$

For the sake of analysis, our implementation of the revenue calculation also outputs the total unsold power for each slot in addition to the total potential revenue if all generated power was sold – for example through the coupling of floating solar output with a non-intermittent electricity source.

3.8 Costs Analysis

Site costs are modelled as the sum of upfront construction costs (capital costs) and a yearly Operations and Maintenance (O&M) cost equal to a percentage of the initial investment. The resulting cumulative cost is expressed in Equation (11), where CC represents the capital costs, $OM\%$ denotes the O&M percentage, and L is the lifetime of the system in years.

$$\text{cumulative_cost}_{year y} = CC \cdot (1 + y \cdot OM\%), \text{ for } y = 1 \text{ to } L \quad (11)$$

Three sources were used to estimate the current capital costs of utility-scale floating solar sites in Switzerland: the most recent World Bank report on the global floating solar market (World Bank Group et al., 2018), a 2019 paper on the topic of optimizing and assessing floating solar systems (Campana et al., 2019), and a 2018 study on the use of floating solar plants in coordination with hydropower (Silvério et al., 2018). System costs are expressed per watt-peak (Wp), which denotes the output of a site under standard test conditions – defined at 25 °C with an air mass coefficient of 1.5 and where the total incoming radiation on the panel equals 1000 watts per square meter (Er et al., 2018). For simplicity, we assume a standard system efficiency of 15%, resulting in 150 Wp per square meter. Multiplying this value by the panel surface area of the respective site yields the power rating in Wp from which we determine capital costs. Table 4 summarizes the values retrieved from our three sources and their conversion to CHF/Wp (exchange rates can be found in Appendix A3). We average these values to establish a capital cost of 1.43 CHF/Wp for floating solar arrays with flat panels (Case 1).

Source	Floating Solar Capital Cost	Value Used for Average (CHF/Wp)
(World Bank Group, ESMAP, & SERIS, 2018)	Range = 0.8 to 1.2 USD/Wp	0.99 (center of range)
(Campana, Wästhage, Nookuea, Tan, & Yan, 2019)	2.35 USD/Wp	2.33
(Silvério et al., 2018)	3.72 BRL/Wp	0.97

Table 4: Retrieved values for floating solar capital costs.

Capital costs rise for floating platforms and anchoring systems as panel tilt increases (Silvério et al., 2018). Therefore, to determine the upfront costs for Cases 3 and 4 (fixed tilt at 12 degrees), we calculate the marginal increase in cost per degree of tilt through a linear regression on data presented in (Silvério et al., 2018) – resulting in an increase of 0.0187 CHF/Wp for each degree ($R^2 = 0.98$) and a total capital cost of 1.65 CHF/Wp for these two cases.

Due to harsh weather conditions in the Swiss alps, Cases 2 and 5 represent hypothetical systems for which no standard products exist. We therefore exclude these cases from our bottom-up costs and investment profiles analyses and instead present their revenue and generation profiles as a motivation for further research and development, along with hypothetical investment profiles if these systems would be built at the same costs as 12-degree panels.

To establish a baseline for the cost profiles of individual sites, yearly O&M costs were set to 2% of capital costs as is the case in the floating solar cost analysis presented in (Campana et al., 2019).

3.9 Investment Profiles

For all sites in our sample, we establish investment profiles by calculating the Levelized Cost of Electricity (LCOE) and the Net Present Value (NPV) under each of the design configurations listed in Table 3. LCOE was computed according to Equation (12), taken from (Darling et al., 2011), while Equation (13) describes our calculation of NPV. Descriptions of the relevant terms and parameters can be found in Table 5.

$$LCOE = \frac{CC + \sum_{n=1}^L \left(\frac{AO}{(1+DR)^n} - \frac{RV}{(1+DR)^n} \right)}{\sum_{n=1}^L \frac{IP \cdot (1-SDR)^n}{(1+DR)^n}} \quad (12)$$

$$NPV = -CC + \sum_{n=1}^L \frac{CF_n}{(1+DR)^n} + \frac{RV}{(1+DR)^L} \quad (13)$$

Term / Parameter	Description	Value Used
CC	Capital Costs	[see Section 3.8]
L	System Lifetime in Years	25
AO	Annual Operations Cost	2% of Capital Costs
DR	Discount Rate	7%, 8%, 10%
RV	Residual Value	10% of Capital Costs
IP	Initial Production	Expected Yearly Generation
SDR	System Degradation Rate	0.5%
CF_n	Cash Flow in Year n	Expected Yearly Revenue * $(1-SDR)^n - AO$

Table 5: Description of terms and parameters used in LCOE & NPV calculations.

Our analysis assumes a system lifetime of 25 years, based on current available technology and typical values found in solar power literature (Ciel & Terre International, 2019) (Khiareddine et al., 2018). To set the system degradation rate, we use results from a 2018 paper stating that reliability studies on floating solar technology have demonstrated rates below half a percent per year for performance loss (Charles Lawrence Kamuyu et al., 2018). Therefore, we assume a yearly degradation of 0.5% to conservatively estimate lifetime generation and revenue.

Finally, we assume that the residual value of a floating solar site is equal to 10% of the initial project cost, as is the case in the analysis presented in (Silvério et al., 2018). Given the investment profiles for individual sites, aggregate profiles for each design configuration were determined by averaging LCOE and summing NPV, respectively.

4 Results

The water body selection criteria described in Section 3.3 results in 82 prospective lakes with a total surface area of 50.1 square kilometers, representing a feasible baseline of high-altitude floating solar sites with hydropower integration options. Figure 7 presents the locations of the sites in our sample along with Swiss agglomerations to illustrate distances to electricity demand centers. Most of the sites in our sample are far from urban areas. However, the associated utility-scale hydro facilities provide grid connections allowing for electricity distribution on a national scale.

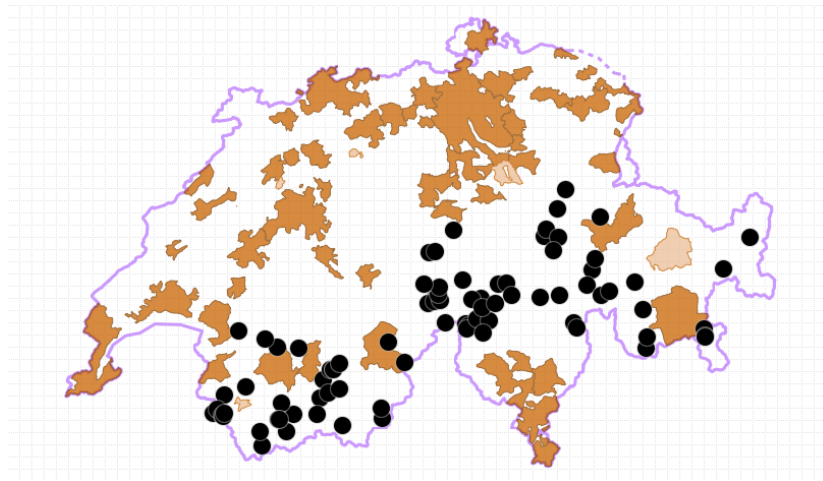


Figure 7: Location of the 82 water bodies in our sample (black dots). Areas shaded in orange represent agglomerations, with data taken from (Federal Office of Topography swisstopo, 2019).

In this section, we focus on Swiss national potential of high-altitude floating solar technology and present aggregate results over the entire sample to address our research questions. Given our bottom-up approach defined in Section 3, individual results for each site depicted in Figure 7 have been established at 15% efficiency for the following three surface area scenarios:

- Scenario 1:* 100% coverage for each water body, conservative upper bounds
- Scenario 2:* 10% coverage for each water body, current system which allows for changes in reservoir depth
- Scenario 3:* 1% coverage for each water body, reference increment / lower bound

These scenarios were chosen as they represent the upper and lower bounds for realistic estimates of technical potential (1% and 100% coverage), with Scenario 2 (10% coverage) providing ballpark results for practical current systems which can deal with large changes in depth. Complete scenario result tables can be found in Appendix A4. In addition, high-resolution individual profiles and links to supporting documents can be accessed on GitHub at <https://github.com/bonesbb/HASPR>, allowing for further research using our data. Supporting documents contain additional information for each water body, including site topography and locations of associated hydropower facilities as illustrated in Figure 8.

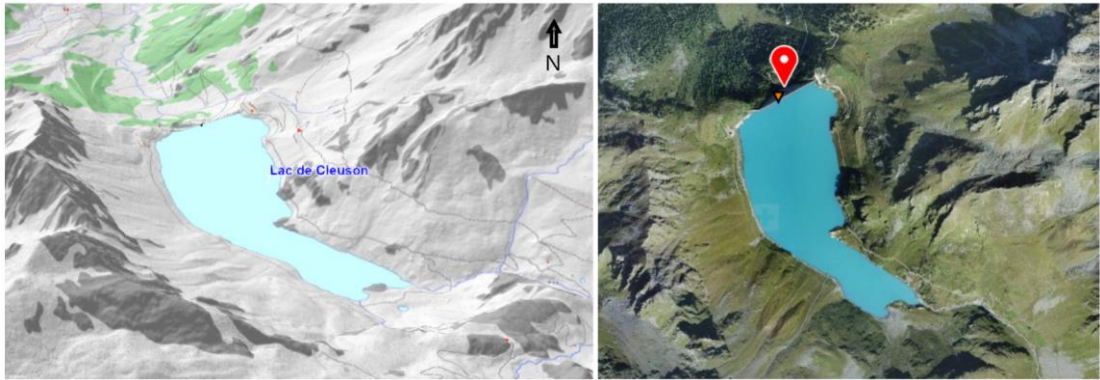


Figure 8: Selection of elements contained in a water body supporting document with Lac de Cleuson as an example. Left: topography. Right: location of an associated hydropower facility.
Image sources: (Federal Office of Topography swisstopo, 2019).

It should be noted that values for generation, costs, and total potential revenue are linear with respect to surface area and panel efficiency. This allows for simple extrapolation of our results to any system efficiency or panel coverage.

4.1 Technical Potential

Conservative aggregate expected generation profiles over our sample of water bodies indicate that the amount of solar energy radiating on Swiss high-altitude lakes is substantial, with an annual average of 1.7 MWh per square meter and over 700 GWh per water body. Figure 9 presents the aggregate floating solar output over the entire sample if system efficiency is 100%. Assuming perfect conversion of solar irradiance into electricity, the total potential energy to

harness is on the scale of Switzerland's entire domestic electricity demand in 2018. In addition, Figure 9 confirms previous research which found that tracking panels in the Swiss alps can harness significantly more energy than flat panels (Durisch & Bulgheroni, 1999). Our results rate annual tracking output at roughly 1.4 times higher than flat panel output for floating solar in the Swiss alps. For comparison, Durisch & Bulgheroni found that tracking panels can harness 1.7 times the output of flat panels at high altitudes in Switzerland. Our optimization of fixed panels at a tilt of 12 degrees for total and winter output yielded very similar results, with over a quarter of the sites in our sample showing no azimuth deviation between the two cases. As a result, annual output with panels fixed at 12 degrees is roughly 1.06 times flat output for both cases. Yearly production for the total optimization is merely 1.0006 times the output when optimized for winter, suggesting that fixed panels should always be optimized for winter production given the higher value of winter electricity in Switzerland. Finally, fixed panels optimized for winter output with a tilt between 35 and 60 degrees can produce 1.09 times flat production, with an average tilt of 45.7 degrees.

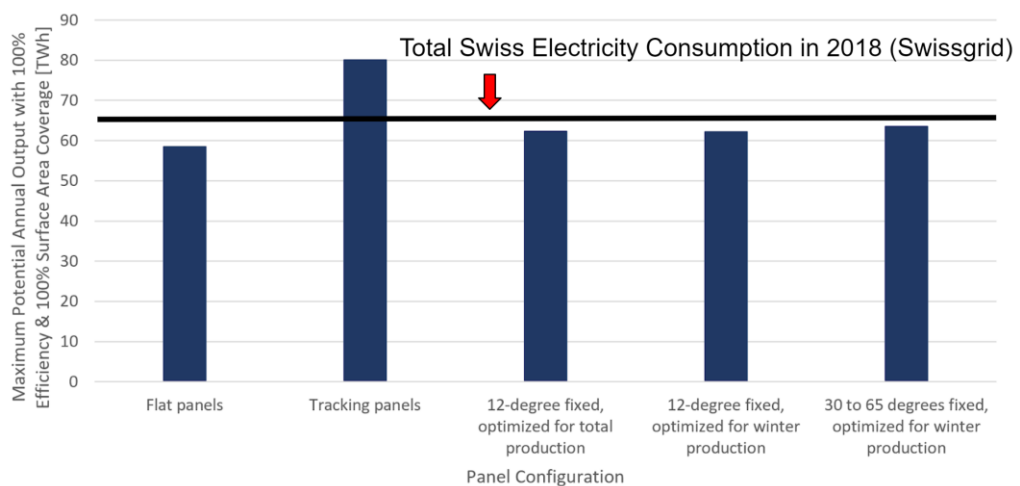


Figure 9: Total annual incoming solar energy across all 82 water bodies under various panel configurations. Total Swiss electricity consumption in 2018 is illustrated as a benchmark. Values assume 100% of surface area is covered by panels operating at 100% efficiency.

With 100% surface area coverage, current systems at 15% efficiency can substitute up to half of Switzerland's nuclear power production in 2018. This scenario implies that high-altitude floating solar technology would account for between 13% and 18% of Swiss electricity generation. The production spread represents the difference in output between flat panels and tracking systems. Across our sample, the corresponding marginal contribution of each

percentage of site surface area stands at 0.13% to 0.18% of Swiss electricity production. For perspective, Figure 10 depicts the nuclear capacity substitution given our 82 water bodies if individual surface area coverage is 100% and 10%, respectively.

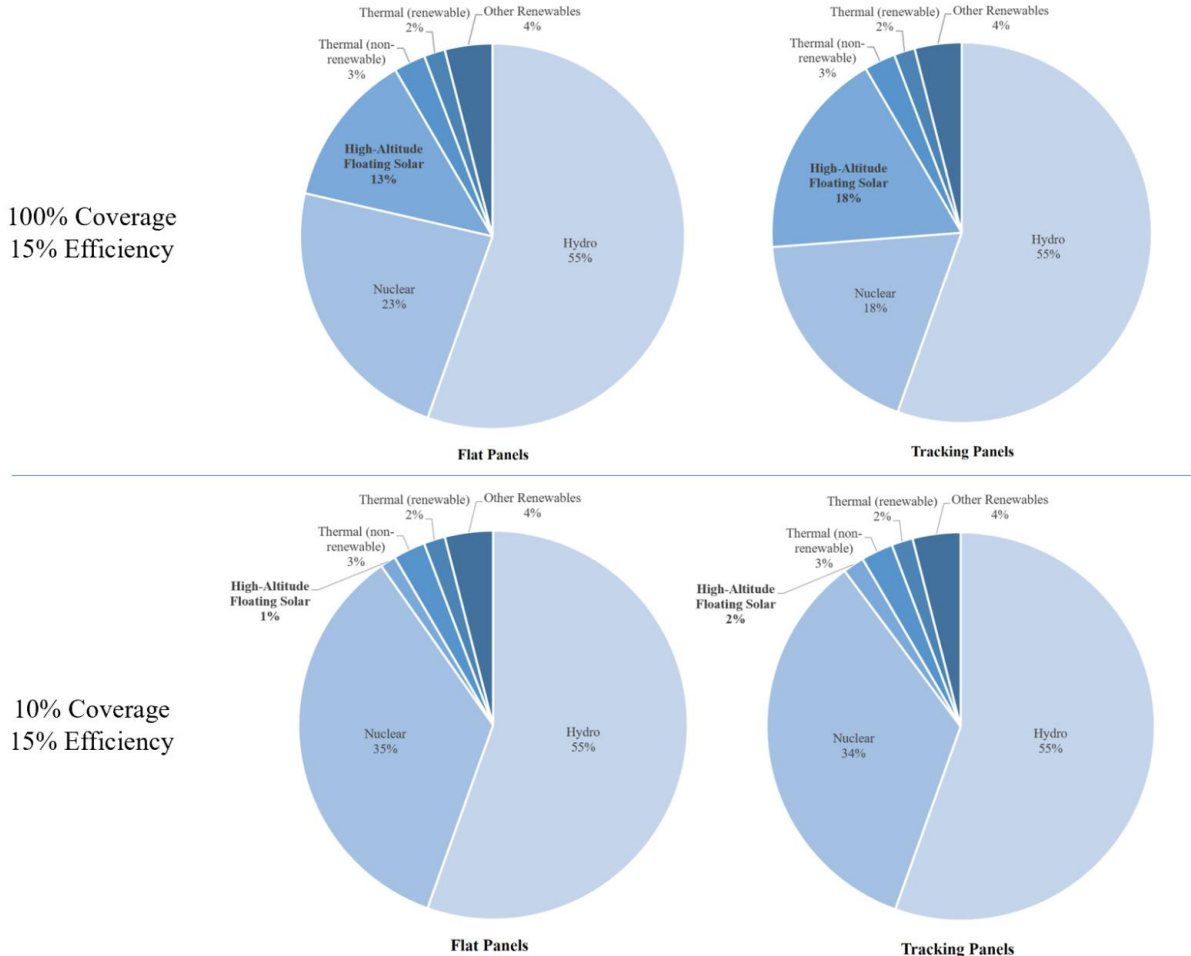


Figure 10: Swiss electricity production by source. Depiction of the potential nuclear capacity substitution with high-altitude floating solar under 100% surface area coverage (top) and 10% surface area coverage (bottom). Panel efficiency is assumed to be 15% and results are shown for the output spread between flat panels (left) and tracking panels (right).

Ranking prospective sites by total expected output reveals that available surface area is the primary factor when determining the technical potential of floating solar power across our sample. Table 6 presents the top 10 sites ranked by total expected annual production along with ranks for surface area and output per square meter for flat panels. *Lac d'Emosson* and *Lac de*

Salanfe are identified as the most interesting prospects, as they are the only two sites among the top 10 for both total output and output per square meter. Total expected annual output stands at 629 GWh for *Lac d'Emosson* and 357 GWh for *Lac de Salanfe*, while 196 kWh and 199 kWh can be harnessed every year per square meter for the two sites, respectively. These values are significantly higher than the averages across all sites considered in this study, which lie at 107 GWh of total output per year and 178 kWh annually per square meter for flat panels.

Total Output Potential Rank	Water Body	Altitude (m)	Surface Area Rank	Output per Square Meter Rank	Annual Flat Output per Square Meter (kWh)	Annual Flat Output at 100% Coverage (GWh)
1	Lac des Dix	2362	1	54	170	679
2	Lac d'Emosson	1920	2	6	196	629
3	Grimselsee	1909	3	55	170	456
4	Lac de Mauvoisin	1969	4	47	175	396
5	Lac de Salanfe	1908	5	4	199	357
6	Oberaarsee	2303	8	23	187	304
7	Lac de l'Hongrin	1250	10	17	191	297
8	Lai da Sontga Maria	1906	6	67	165	293
9	Stausee Mattmark	2195	7	69	163	284
10	Lago Ritóm	1850	11	25	185	271

Table 6: Top 10 sites in our sample ranked by total expected annual production. *Lac d'Emosson* and *Lac de Salanfe* are highlighted as the only 2 sites among the top 10 for both total output and output per square meter.

As presented in Figure 11, our results confirm that higher tilt angles can be used to increase solar production in winter at high altitudes. While tracking systems dominate all other configurations, panels optimized for winter output with tilts between 30 and 65 degrees can harness an average of 87% of tracking production from November to February. Compared to flat panels, these high tilt angles allow output to be shifted from summer months to the winter season while simultaneously increasing total annual production.

Despite the increase in winter generation with higher tilts, high-altitude floating solar sites still produce most of their power in summer. Figure 12 illustrates the breakdown between yearly and winter production for each panel configuration. A maximum of 35% of total output can be produced during winter months with tilts between 30 and 65 degrees, compared to 30% for flat panels. Integration with the associated hydropower facilities could provide seasonal storage to shift even more production from summer to winter.

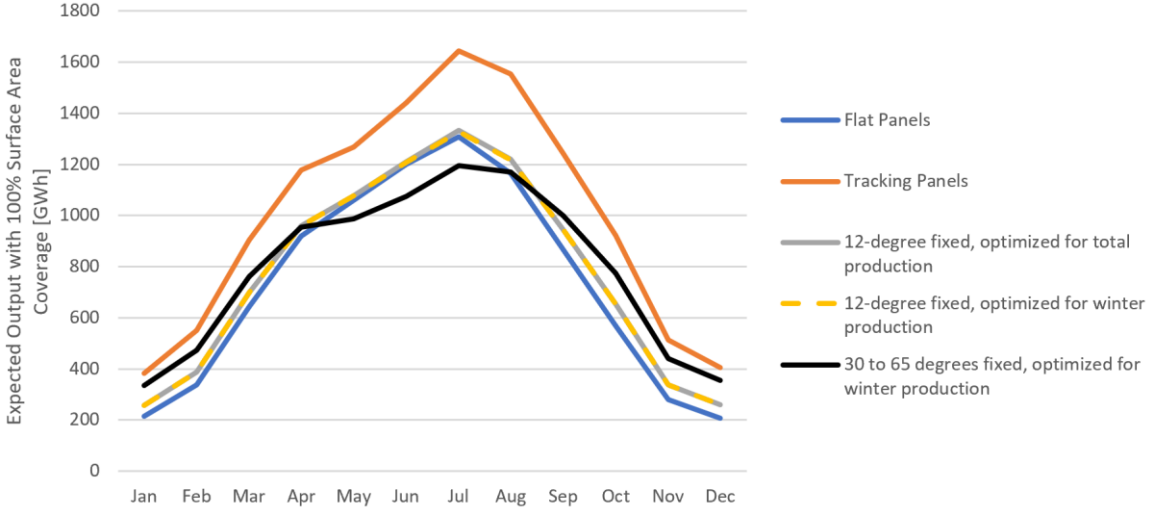


Figure 11: Total expected floating solar output under multiple design configurations assuming panel surface area equals 100% of the respective water body's surface area and 15% efficiency.

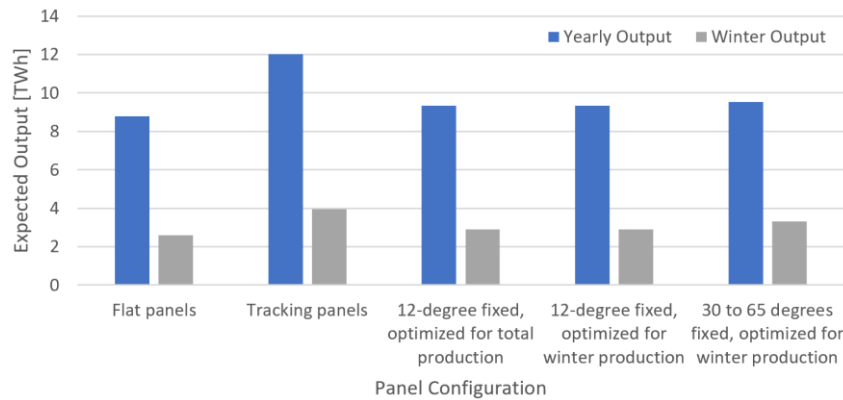


Figure 12: Expected yearly vs. winter output under multiple design configurations assuming panel surface area equals 100% of the respective water body's surface area and 15% efficiency.

As illustrated in Figure 13, higher variances in historic output are observed as panel tilt increases, with tracking panels exhibiting significantly higher normalized variance than any other configuration. In addition, lower variances are observed in winter for all cases besides fixed panels between 30 and 65 degrees. As a result, the lowest uncertainty in high-altitude floating solar production is achieved with flat panels, where the annual lower bound for 30-minute slots stands at 18% (with 95% confidence). In contrast, the highest uncertainty in output is realized with tracking panels, with a corresponding annual lower bound of 6%.

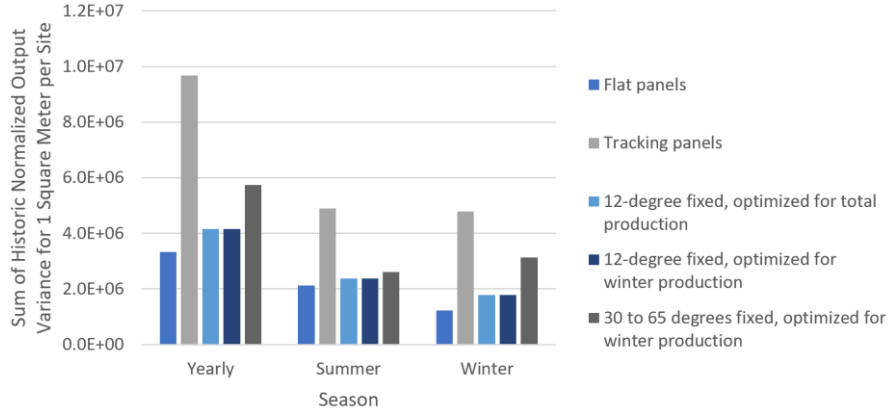


Figure 13: Sum of historic normalized output variance for 1 square meter of each site in 30-minute slots.

4.1.2 Addressing the Swiss Temporal Supply/Demand Mismatch

With 100% surface area coverage and 15% efficiency, our sample of 82 water bodies can alleviate up to a third of the temporal discrepancy between electricity production and consumption in Switzerland. As Figure 14 illustrates, a larger portion of the mismatch can be addressed as panel tilt increases. These results confirm the potential for high-altitude solar arrays to relieve pressure on Switzerland's electricity market in winter. Moreover, we find that high tilts are not explicitly needed to significantly address the temporal supply/demand discrepancy. Flat panels on our sample of water bodies can account for 85% of the mismatch offset achievable with fixed panels between 30 and 65 degrees. Marginally, covering an additional 1% of each water body's surface area has the potential to decrease the temporal deficit by roughly 0.4%.

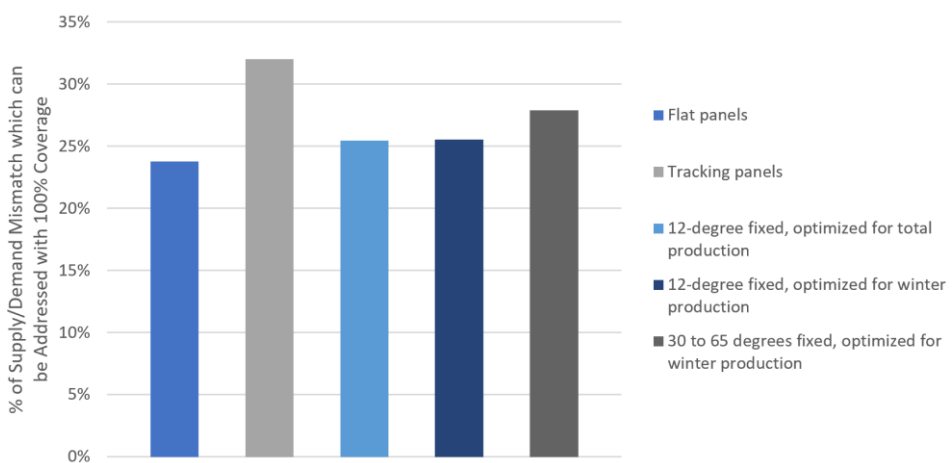


Figure 14: Percentage of Swiss temporal supply/demand mismatch which can be addressed under multiple design configurations, assuming 100% coverage and 15% efficiency.

4.1.3 CO₂ Offset Analysis

If 15%-efficient floating solar panels would cover the entire 50.1 square kilometers of our sample, the resulting annual reduction in CO₂-equivalent emissions would be roughly equivalent to two thirds of total European emissions from coal power in 2016. Figure 15 presents the CO₂ offsets for each panel configuration in this scenario. Once again, tracking panels dominate, potentially reducing annual CO₂-equivalent emissions by over 1 gigaton. For comparison, flat panels in this case would decrease emissions by roughly 717 megatons per year. As a reference, between 7.2 and 10.3 megatons of CO₂ could be offset every year for each percentage of water body coverage. However, it should be noted that these results do not take the full lifecycle of floating solar technology into account. Instead, these figures represent annual CO₂-equivalent offsets as a result of substituting clean electricity for non-zero emissions sources, assuming the floating solar arrays have already been built.

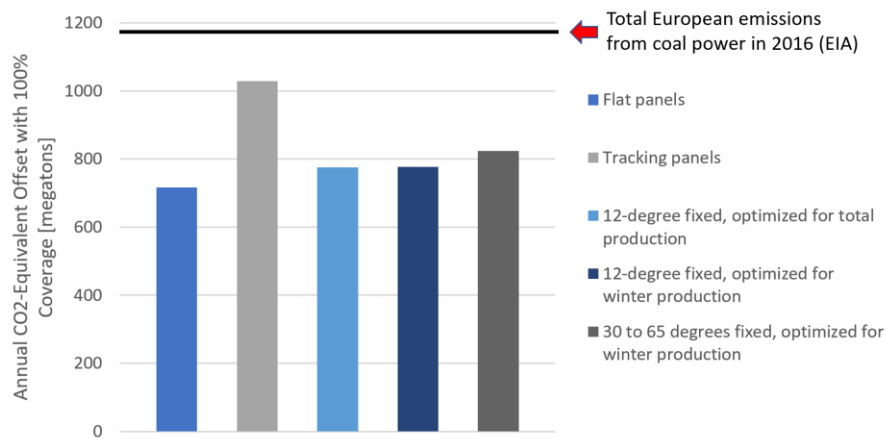


Figure 15: Annual CO₂-equivalent offset if high-altitude floating solar power is used as a substitute for current non-zero emissions sources (including imports). Total European emissions from coal power in 2016 is illustrated as a benchmark and is sourced from (U.S. Energy Information Administration, 2019).

4.2 Economic Potential

Despite substantial revenue potential on the Swiss day-ahead market, high-altitude floating solar power is currently not economically viable without subsidies given the cost estimates outlined in Section 3.8 (assuming power is sold at the time of generation). Although tracking panels and designs with tilts between 30 and 65 degrees boast significantly higher energy yields than flat arrays and panels fixed at 12 degrees, these systems would still be unprofitable on the free market if they could be built at the same costs as 12-degree arrays. Consequently, a 50-60% reduction in the capital costs reported in (World Bank Group et al., 2018) is required for economic viability of flat panels across our sample. However, these results do not account for reduced grid connection costs which could be achieved by taking advantage of existing grid infrastructure provided by associated hydropower plants. In Section 4.2.1, we present a complete overview of cost targets which would result in profitable projects (NPV greater than 0) for various panel configurations.

Figure 16 illustrates the total potential annual revenue at 15% efficiency with 100% coverage across our sample, while Figure 17 displays the corresponding monthly profiles for each configuration case. Following the trend in total production, increased yearly revenues can be attained with higher panel tilts, with an annual total potential revenue ranging between CHF 388 million for flat panels and CHF 551 million for tracking systems. Furthermore, the difference between bid and potential revenue shrinks as surface area coverage increases, with bid revenue equal to roughly 85% of potential revenue for 1% coverage and approximately 98% of potential revenue for 10% coverage. Placing panels on 100% of the available surface area results in essentially no difference between bid and potential revenue.

Given the cost analysis described in Section 3.8, total capital costs for floating solar installations with 100% coverage under flat and 12-degree tilts correspond to the cost of installing 5 to 6 new coal power plants (assuming a cost of roughly CHF 2 billion for a GW-scale coal plant). For reference, this range is equivalent to between CHF 107 million and CHF 124 million for each percentage of surface area coverage. Since our cost model is linear with respect to surface area, the greatest economic viability is achieved by selecting sites with the highest energy output per square meter.

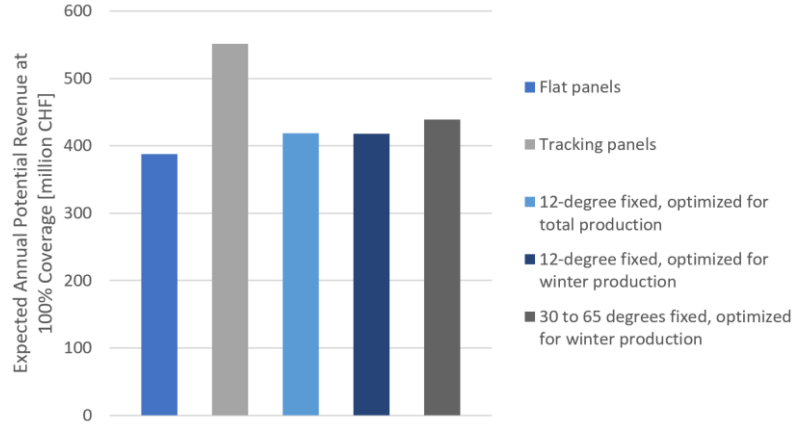


Figure 16: Total expected annual potential revenue under multiple design configurations with 100% coverage and 15% efficiency. Values assume that power is sold at the time of generation on the Swiss day-ahead market.

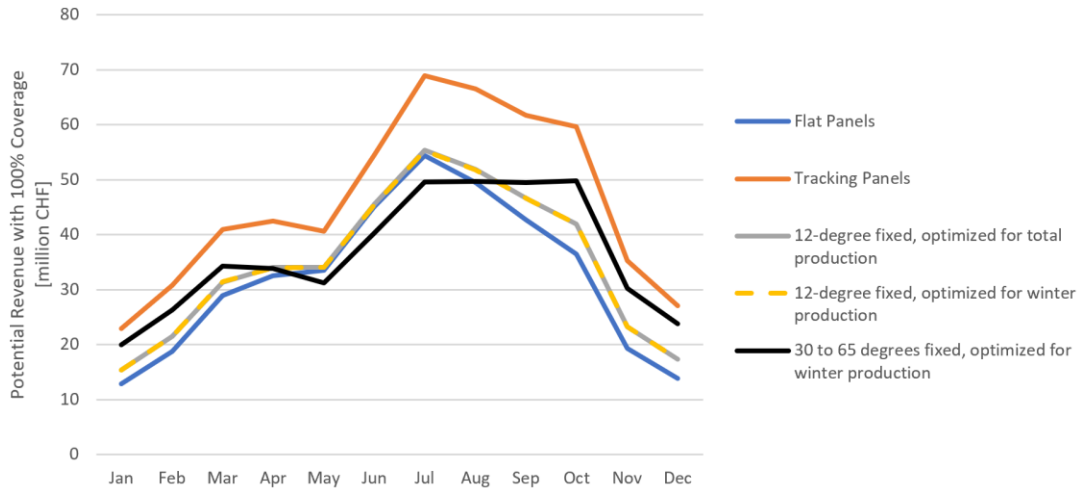


Figure 17: Potential total revenue profiles for multiple design configurations with 100% coverage and 15% efficiency. Values assume that power is sold at the time of generation on the Swiss day-ahead market.

Ranking locations by energy efficiency (Wh/m^2) is equivalent to ranking sites via our LCOE results. Following this method, Table 7 presents the top 10 sites in our sample ranked by economic viability. *Lac d'Emosson* and *Lac de Salanfe* are identified once again as top sites, both technically and economically. As a key insight, our results indicate a general tradeoff between economic viability and technical potential (with the notable exceptions of *Lac d'Emosson* and *Lac de Salanfe*). This tradeoff stems from relatively small surface areas for most sites with high economic viability rankings, resulting in lower technical potential.

Economic Viability Rank	Water Body	Altitude (m)	Surface Area Rank	Annual Flat Output per Square Meter (kWh)	Annual Flat Output at 100% Coverage (GWh)
1	Lac Supérieur de Fully	2130	46	210	43
2	Stausee Gibidum	1436	45	209	43
3	[Vissoie unnamed 1]	1119	79	202	2
4	Lac de Salanfe	1908	5	199	357
5	Zmuttbach	1968	63	197	8
6	Lac d'Emosson	1920	2	196	629
7	[Spina (Isola) unnamed]	1191	70	193	5
8	[Peccia (Sambuco) unnamed]	1032	74	192	3
9	[Châtelard-Barberine unnamed]	1115	75	192	3
10	[Châtelard-Vallorcine unnamed 1]	1119	80	192	2

Table 7: Top 10 sites in our sample ranked by economic viability (equivalent to lowest LCOE and highest output per square meter). *Lac d'Emosson* and *Lac de Salanfe* are highlighted as the only 2 sites among the top 10 for both technical potential and economic viability.

Note: Locations of unnamed water bodies can be found in Appendix A2.

LCOE for flat panels range from 0.74 to 3.8 CHF cents per kWh, representing lifetime costs assuming a discount rate between 7 and 10 percent. Panels fixed at 12 degrees are relatively more expensive, with LCOE values roughly 9% higher than those calculated for flat panels. This implies that flat arrays are the most economically viable design case for current systems. Assuming the same costs as 12-degree designs, tilting panels between 30 and 65 degrees results in a 6% increase in LCOE compared to flat arrays. Of the configuration cases explored in this study, only tracking panels have lower average LCOE values than flat systems, lying 16% below the levelized cost for horizontal arrays if they can be built at the same costs as 12-degree panels.

All LCOE results are above Swiss average day-ahead electricity prices, resulting in negative NPV values over 25 years of system lifetime for all water bodies and design configurations. As a result, this analysis implies that Swiss high-altitude floating solar power is currently not economically viable without taxpayer money if power is sold at the time of generation on the Swiss day-ahead market. Taxpayers in Switzerland would have to pay a total of between CHF 87 million and CHF 105 million per percentage of surface area coverage, equivalent to between CHF 10.3 and CHF 12.5 per resident, for 25 years of floating solar power.

4.2.1 Cost Targets

Table 8 presents cost targets needed for high-altitude floating solar arrays to be lucrative when power is sold at the time of generation. As a baseline, if capital costs reach between 0.41 CHF/Wp and 0.5 CHF/Wp, flat panels would be economically viable without subsidies. For tracking systems, cost targets range between 0.57 CHF/Wp and 0.7 CHF/Wp for economic viability. Panels with a fixed tilt of 12 degrees would be profitable if costs are below 0.53 CHF/Wp, while tilts of 30 to 65 degrees require a cost target of 0.55 CHF/Wp. Overall, current capital costs would have to decrease by roughly 50-60% for Swiss high-altitude floating solar technology to be profitable under our assumptions.

Cost Target (CHF/Wp)	Implication
0.5	25 of out 82 sites would be economically viable
0.47	Sample as a whole would be economically viable (sum of NPV > 0)
0.41	All 82 sites would be economically viable

Table 8: Baseline cost targets to achieve various levels of economic viability with flat panels. Values assume no government subsidies and a discount rate of 7%.

5 Discussion & Implications

With the ability to provide large amounts of power and significantly address the temporal supply/demand mismatch, emerging floating solar technology has the potential to strongly contribute to a post-nuclear 100% renewable Swiss electricity grid. Our technical results provide compelling motivation for the development of suitable alpine floating solar installations in Switzerland, particularly if storage and grid connections are available through hybrid floating solar / hydro systems. In addition, the environmental benefits of modular and reversible systems along with significant CO₂ offsets make a strong case for pursuing this technology under the vision of a sustainable future. However, the floating solar industry is still in its infancy and further research is required to achieve the significant reduction in capital costs needed for economic viability without subsidies or storage. This study offers individual generation profiles and cost criteria for successful projects on 82 suitable water bodies, thereby providing the foundations for the next steps in exploiting floating solar technology in Switzerland.

To be economically viable without taxpayer money, either costs must significantly decrease, or power needs to be sold at higher prices – for example through storage. Our model of capital costs includes expenses related to building utility-scale grid connections for each prospective site. Sharing this infrastructure with associated hydropower plants may result in significantly lower construction costs, adding to the expected decrease in costs as the floating solar industry matures. Integrations with existing hydro utilities may also present opportunities for O&M synergies, with the benefit of existing on-site personnel and road access. Additionally, any increases in efficiency would have a positive effect on cost targets. The assumed 15% efficiency may be considerably lower than what is achievable given the low operating temperatures and the natural cooling effect of water. Finally, combining high-altitude floating solar with storage technology would increase site profitability by enabling the sale of generated power at higher prices. This may be achieved through integration with associated hydro pumped-storage facilities.

For the proliferation of high-altitude floating solar power in Switzerland, further research is needed to determine the most suitable design configuration. Although current products are

capable of withstanding heavy winds and snowfall (Ciel & Terre International, 2019), snow-covered panels result in decreased efficiency (Awad et al., 2018). This implies lower production during winter months, precisely when it is desirable to maximize output to alleviate the temporal supply/demand mismatch. Current research is exploring the use of hydrophobic and icephobic coatings to avoid snow cover, while the ability of high-tilts to significantly reduce the accumulation of snow on solar panels has been demonstrated (Andenæs et al., 2018). The use of bifacial panels is a particularly interesting topic to explore, as such systems could exploit reflections from the water surface to boost generation while using high tilts to increase winter output. This study concludes that flat panels are currently the most economically viable option. However, at the right costs, higher tilts and tracking systems would be able to make a larger impact and produce more valuable electricity in winter. On an annual basis, tracking panels produce roughly 40% more power than flat panels, while fixed-tilts increase generation by 6% and 9% for 12-degree panels and tilts between 30 and 65 degrees, respectively. The increased investment needed for these systems may be justified by gains in production, especially considering the importance of adding winter capacity. Technically speaking, tracking panels and tilts between 30 and 65 degrees are the most promising configurations we investigated. However, the application of such systems in harsh conditions at high-altitude requires further research.

The prospect of integrating floating solar panels with hydropower plants is especially interesting in Switzerland, where glacier melting due to climate change has resulted in uncertainty in future water resources for hydro utilities (Beniston, 2012). Hybrid solar/hydro systems can help stabilize production and mitigate climate risks, with interesting use cases in peaking plants, load balancing, energy arbitrage, and ancillary grid services. Furthermore, floating solar output could be used to compensate for times when water storage levels are low, providing valuable relief for hydro operators. This would result in less reliance on imports during the filling season and increased savings of hydro capacity for the winter. In addition, reduced evaporation rates on hydro reservoirs with floating solar implies further valuable water savings. Hybrid integration of floating solar with hydropower is still at an early stage (World Bank Group et al., 2018). However, incentives are strong for Swiss hydro managers to pursue floating solar systems using their existing substation infrastructure given the potential benefits and strategic importance of integration, especially as the floating solar industry matures. As an example, *Statkraft* (a large Norwegian hydro producer) is optimistic about complementing

hydro production with floating solar and is currently pursuing pilot integrations in Albania (CleanTechnica, 2019). This presents an interesting learning opportunity for Swiss hydro managers. In addition, the increased revenue potential from floating solar combined with hydro storage (enabling power sales at higher prices) also provides further prospects for viable business cases.

Besides cost barriers and engineering, the implementation of high-altitude floating solar in Switzerland faces several challenges. Public opinion may be against the further construction of energy infrastructure on alpine lakes, especially since many of the water bodies in our sample are popular sightseeing destinations. Previous research on the risks of developing photovoltaic projects in the Swiss alps has found that project acceptance relies heavily on contributions to the local economy, with transparent and regular information flows between stakeholders as a key driver of project approval (Díaz & Van Vliet, 2018). Díaz & Van Vliet also found that the high complexity of administrative processes related to developing new renewable projects pose a significant implementation risk. Given the existing local relationships and permits held by hydropower facilities, the path of least resistance for implementing high-altitude floating solar in Switzerland is likely to be through associated hydro operators.

Overall, our results suggest that high-altitude floating solar technology should be on the radar of the Swiss government and energy industry. The prospect of utility-scale production and homogenous spaces presents the technology as a solid option for large-scale expansions in Swiss solar capacity. Additionally, given proper funding, Switzerland can take advantage of its engineering prowess and potentially position itself as a key innovator in the high-growth floating solar industry. Specifically, Swiss hydropower managers have much to gain by incorporating floating solar systems. Pilot projects on *Lac d'Emosson* and *Lac de Salanfe*, the top 2 sites identified in our analysis, would be an appropriate starting point for the roll-out of high-altitude floating solar arrays in Switzerland. If such systems are deemed feasible, the expected decrease in capital costs over time may allow viable sites to overcome the tradeoff between technical and economic potential, opening the door for utility-scale proliferation of the technology to help Switzerland reach its energy targets.

5.2 Limitations & Further Research

The models and analysis scripts developed in the HASPR environment were checked for robustness by comparing test outputs to values calculated by hand. In addition, generation profiles have been validated by comparing average annual output to published results. The sample's yearly average of 133 W/m^2 is consistent with data presented in (Kahl et al., 2019) and confirms this study's conservative approach. However, the primary limitation of our POA model lies in the spatial resolution of the meteorological data sets. At roughly 5 km, the pixel resolution is too high to take topographic shading into account for many of the water bodies, potentially distorting output results. Furthermore, the model's assumptions of isotropic diffuse radiation and constant system efficiency (assuming no panel snow cover and temperature effects) limit the precision of the values presented herein. Limitations also arise from our available surface area data. Hydro storage reservoirs vary in depth and surface area over time, while only one value for surface area is available from our swisstopo source. Moreover, due to shading, 100% surface area coverage is not possible with tilted panels, implying that the maximum technical potential for tilted and tracking arrays is optimistic. Finally, the future development of electricity prices has not been considered in this study. If prices fall, high-altitude floating solar may not be economically viable in Switzerland even if the cost targets we presented are achieved.

Further engineering research is needed to develop low-cost and robust systems capable of dealing with large changes in depth and harsh alpine conditions. Pilot studies and measurements on individual water bodies would allow for the validation of the technical potential presented in this study. In addition, how exactly floating solar should be integrated with hydropower and the role of the technology in the Swiss electricity mix still needs further investigation. For example, floating solar generation profiles may be added to existing Swiss capacity expansion models to determine the most effective use of the technology while taking future prices and storage options into account. Furthermore, the application of floating solar to river basins and lower altitude lakes (with or without existing hydro infrastructure) may be promising and warrants further research. Finally, the CO₂ offset analysis presented in this study does not take the full lifecycle of floating systems into account. Therefore, a lifecycle analysis should be conducted to determine the full extent of the environmental impact of these systems.

6 Conclusion & Outlook

The technical potential and environmental benefits of high-altitude floating solar technology have been demonstrated to be highly promising for the Swiss electricity mix. Key barriers to implementation include substantial capital costs, which are currently still too high for economic viability without subsidies or storage, and engineering challenges in tailoring the technology to Swiss alpine water bodies. However, Switzerland is well-poised to exploit high-altitude floating solar power in the near future if investments are made in research and development of utility-scale projects. Costs are expected to drop and the added value for Switzerland's hydropower sector presents floating solar as a strategic opportunity to reduce risk and reliance on imports.

This study builds on current research revealing the remarkable potential of Swiss high-altitude solar power by demonstrating the merits of using alpine water bodies to dramatically increase domestic solar capacity while overcoming the key barrier of land access. With HASPR, we also provide a quantitative analysis framework for site assessment, along with high-resolution data on 82 prospective locations for further research.

Assuming implementation barriers can be overcome, Switzerland is set to significantly address its nuclear phase-out, protect its electrical sovereignty, and solidify its crucial position in the European grid through the application of floating solar coupled with hydropower at high altitudes. This undertaking would represent a key integration step in the direction of a net-zero emissions energy system. Given the upside and pace of the industry so far, it is reasonable to imagine a scenario where the scale of Swiss high-altitude floating solar is significantly contributing to a post-nuclear grid by 2050.

A Appendix

A1 Complete List of HASPR Scripts & Documentation

All HASPR scripts and result tables can be found at <https://github.com/bonesbb/HASPR> along with detailed documentation in the repository's README.md file and code commentary. Questions regarding the code and its use can be addressed to eyring.nick@gmail.com.

Core Scripts:

datascrape.py	Script to extract light-weight data sets and merge files from large NetCDF4 directories.
haspr.py	Background script/library containing classes, functions, and global variables.

Generation Scripts:

batch_check.py	Checks if batches have successfully run. Outputs incomplete batch list.
batch_submission_bf.py	Script for setting up brute force batch jobs for fixed-tilt optimizations on Euler.
batch_submission_opt.py	Script for setting up batch jobs for fixed-tilt calculations on Euler.
main_euler_fixed.py	Main script for Euler fixed-tilt batches. Sets parameters, runs models, and dumps data.
main_euler_flat.py	Main script for Euler flat batches. Sets parameters, runs models, and dumps data.
main_euler_tracking.py	Main script for Euler tracking batches. Sets parameters, runs models, and dumps data.
optimization_results.py	Determines optimum fixed-tilt positions given directories of brute force output.
organize_batch_output.py	Copies files from batch output to corresponding historic profile directories.

Processing Scripts:

global_remove_leap.py	Removes leap days for a global panel configuration case.
lower_resolution.py	Converts data series to hourly, daily, or monthly resolution.
remove_leap_days.py	Script to remove leap days from a directory of generation profiles.

Analysis Scripts:

average_aggregate_revenue.py	Outputs average bid and potential revenue given a directory of aggregate revenue profiles.
average_individual_revenue.py	Script which averages individual revenue profiles from historic data.
co2_offset.py	Calculates CO2-equivalent offset given generation profiles.
expected_output_analysis.py	Computes aggregate lower bounds and historic variance given a directory of individual expected output.
expected_site_output.py	Script to calculate expected output for one site given a directory of historic profiles.
global_expected_site_output.py	Script to calculate expected output for all sites under a design configuration.
lifetime_costs.py	Calculates costs given a CSV file of sites, panel surface area, and tilt angles.
lifetime_revenue.py	Calculates yearly and cumulative revenue for system lifetime given a directory of revenue profiles.
NPV_LCOE.py	Computes the NPV and LCOE given lifetime costs/revenues and expected generation profiles.
revenue.py	Outputs revenue profiles for all generation profiles in a given directory.
sum_individual.py	Script to calculate annual sums given generation profiles.
supply_demand_mismatch.py	Computes the potential alleviation of supply/demand mismatches given generation profiles.
total_expected_output.py	Script to calculate generation profiles in Wh from a directory of profiles in Wh per square meter.
total_generation_profile.py	Script to calculate aggregate generation profiles given surface areas.

A2 Full Water Body Sample and Collected Attributes

Note: Full tables are available at <https://github.com/bonesbb/HASPR>.

Site ID	Name	Canton	Altitude (m)	Coordinates (WGS 84)	Surface Area (m ²)	Associated Hydro Installations (ZE-Nr.) *
1	Lago Bianco	GR	2234	46°24'18.518"N 10°01'10.443"E	1431937	700200, 700100, 700300, 700400
2	Lac des Dix	VS	2362	46°03'26.019"N 7°23'48.246"E	3999336	505000, 504950, 505100
3	Zmuttbach	VS	1968	46°00'27.630"N 7°42'26.388"E	39741	504600, 504700
4	Grimselsee	BE	1909	46°33'58.305"N 8°18'14.370"E	2687955	200300, 200100, 200400, 200800
5	Oberaarsee	BE	2303	46°32'37.302"N 8°15'32.158"E	1626936	200200, 200100
6	Triebtenseewli	BE	2365	46°33'09.131"N 8°17'52.441"E	96595	200200
7	Totesee	VS	2160	46°33'37.864"N 8°20'24.409"E	193451	200400
8	Rätterichsbodensee	BE	1767	46°35'07.786"N 8°19'40.579"E	657746	200500, 201100, 200800, 201300, 200600
9	Gelmersee	BE	1849	46°36'56.434"N 8°19'48.164"E	616993	200400, 200800
10	Lac de Mauvoisin	VS	1969	45°58'46.819"N 7°21'12.761"E	2255726	505300, 505400
11	Lac de Moiry	VS	2248	46°07'44.768"N 7°34'14.213"E	1309592	503200
12	Stausee Mattmark	VS	2195	46°02'16.908"N 7°57'36.736"E	1741439	501500, 501600
13	Lac de Salanfe	VS	1908	46°08'26.565"N 6°57'30.465"E	1795618	507700, 507600, 507500
14	Lac du Vieux Emosson	VS	2225	46°03'42.913"N 6°53'23.662"E	545561	506900, 506800, 506850, 506700
15	Lac d'Emosson	VS	1920	46°04'46.590"N 6°55'03.403"E	3214380	506900, 506800, 506850, 506700
16	Lac des Toules	VS	1809	45°55'08.903"N 7°11'55.159"E	599167	505900
17	Gigerwaldsee	SG	1331	46°54'52.718"N 9°22'24.901"E	689511	104700, 104600
18	Limmerensee	GL	1855	46°50'06.476"N 9°00'52.678"E	1340348	400100, 400200, 400250, 400400, 400050
19	Muttsee	GL	2474	46°51'49.489"N 9°01'41.577"E	410167	400100, 400050
20	Lag da Pigniu	GR	1447	46°49'48.710"N 9°06'12.977"E	390001	101000
21	Lai da Marmorera	GR	1676	46°30'02.559"N 9°38'09.970"E	1369543	103100, 103200
22	Lägh da l'Albigna	GR	2162	46°19'47.530"N 9°38'51.736"E	1258106	701200, 701000, 701100, 700800, 701400
23	Lai dad Ova spin	GR	1630	46°40'08.709"N 10°09'32.022"E	351190	800800
24	Lac de l'Hongrin	VD	1250	46°25'27.784"N 7°03'03.084"E	1552993	509100
25	Lago Dei Cavagnöö	TI	2310	46°27'16.427"N 8°30'05.141"E	476416	602500
26	Lago di Robièi	TI	1940	46°26'42.852"N 8°31'00.384"E	246134	602600, 602500
27	Lago del Zött	TI	1940	46°25'59.078"N 8°30'10.549"E	148255	602600
28	Lago Del Naret	TI	2310	46°28'38.474"N 8°34'08.384"E	731588	602500
29	Lago Del Sambuco	TI	1461	46°27'48.400"N 8°38'59.169"E	1109119	602400
30	Mattenalpsee	BE	1874	46°37'49.606"N 8°14'04.222"E	186439	200500
31	Lac Supérieur de Fully	VS	2130	46°10'42.715"N 7°05'38.072"E	203904	505600
32	Lagh da Palü	GR	1923	46°22'23.285"N 10°01'31.567"E	53615	700100, 700300
33	Lac de Cleuson	VS	2179	46°06'27.489"N 7°19'22.793"E	478894	504300
34	Lago della Sella	TI	2256	46°33'48.593"N 8°35'54.343"E	450778	600050, 600200, 600100
35	Griessee	VS	2386	46°27'27.473"N 8°22'14.130"E	636908	500100
36	[Löbbia unnamed]	GR	1416	46°22'35.312"N 9°39'29.383"E	29232	701200, 701000, 701100, 700800
37	[Palü unnamed]	GR	1923	46°22'18.512"N 10°01'27.150"E	3196	700100, 700300
38	[Ferpècle unnamed]	VS	1891	46°03'28.271"N 7°33'01.451"E	11174	504800
39	Zervreilasee	GR	1857	46°34'13.045"N 9°06'13.332"E	1564848	101100
40	[Fionnay unnamed 1]	VS	1484	46°02'02.917"N 7°18'17.297"E	29255	505300, 505000
41	[Fionnay unnamed 2]	VS	1491	46°02'00.911"N 7°18'31.832"E	17474	505300, 505000
42	Bortelsee	VS	2464	46°17'15.158"N 8°06'28.216"E	136491	501375, 501350
43	[Pallazuit unnamed]	VS	1327	45°58'54.120"N 7°11'20.977"E	15866	505900
44	Lai da Curnera	GR	1955	46°37'37.989"N 8°42'47.885"E	793864	100200
45	Lai da Nalps	GR	1904	46°37'53.009"N 8°45'47.373"E	901199	100200
46	Lai da Sontga Maria	GR	1906	46°34'32.128"N 8°47'43.351"E	1773494	100200
47	[Safien Platz unnamed 1]	GR	1294	46°40'47.942"N 9°19'00.192"E	29814	101200
48	Rabiusa	GR	1147	46°43'53.721"N 9°20'18.153"E	38051	101200
49	[Safien Platz unnamed 2]	GR	1720	46°36'56.418"N 9°16'42.940"E	36511	101200
50	Sanetschsee	VS	2033	46°21'24.504"N 7°17'39.240"E	284234	203600
51	Lago d'Isola	GR	1602	46°26'59.160"N 9°11'16.088"E	363253	601400
52	[Spina (Isola) unnamed]	GR	1191	46°25'43.141"N 9°12'27.602"E	25958	601400
53	Arnesee	BE	1541	46°23'20.605"N 7°13'01.871"E	449916	508700
54	Lago di Lucendro	TI	2134	46°33'43.358"N 8°32'27.926"E	542675	600100
55	[Airolo unnamed]	TI	1129	46°31'33.916"N 8°36'16.108"E	47827	600100
56	[Pradella unnamed]	GR	1141	46°48'14.232"N 10°20'06.790"E	33245	801000
57	[Châtelard-Vallorcine unnamed 1]	VS	1119	46°03'07.796"N 6°57'02.065"E	10822	507100, 506700
58	[Châtelard-Vallorcine unnamed 2]	VS	1515	46°02'53.915"N 6°57'26.714"E	24012	507100, 506700
59	[Vissoie unnamed 1]	VS	1119	46°12'42.622"N 7°35'06.243"E	11086	503300
60	[Vissoie unnamed 2]	VS	1560	46°09'09.184"N 7°37'16.028"E	22469	503300, 503200
61	Oberer Murgsee	SG	1819	47°02'21.174"N 9°09'14.903"E	196690	403000
62	Göschenenalpsee	UR	1792	46°38'43.280"N 8°29'00.990"E	1304567	300400
63	Sufnersee	GR	1398	46°33'59.088"N 9°22'08.944"E	823086	102100
64	Lai da Seara	GR	1080	46°35'14.964"N 9°25'15.253"E	67821	102100
65	Melchsee	OW	1891	46°46'14.847"N 8°16'20.967"E	507012	303800, 303650
66	Tannensee	OW	1976	46°46'25.190"N 8°18'23.212"E	339608	303800, 303650
67	Lago di Luzzzone	TI	1606	46°34'00.390"N 8°58'36.032"E	1401350	601200
68	Lago Ritón	TI	1850	46°32'26.225"N 8°41'25.633"E	1461650	600400
69	Lac de Tseuxier	VS	1774	46°21'01.878"N 7°25'50.353"E	829589	503500, 503700
70	Bannalpsee	NW	1586	46°52'04.059"N 8°25'47.114"E	157598	303300

...

Site ID	Name	Canton	Altitude (m)	Coordinates (WGS 84)	Surface Area (m ²)	Associated Hydro Installations (ZE-Nr.) *
71	Lai da Burvagn	GR	1116	46°37'16.944"N 9°35'13.116"E	47529	103200
72	Lag da Breil	GR	1254	46°46'17.363"N 9°04'15.743"E	62743	100300, 101000
73	Stausee Gibidum	VS	1436	46°22'26.493"N 8°00'11.565"E	204456	501200
74	Turtmannsee	VS	2176	46°10'07.068"N 7°41'34.562"E	98406	502800, 503200, 502600
75	Stausee Garichti	GL	1622	46°57'20.532"N 9°05'58.445"E	152984	401500
76	Illsee	VS	2359	46°15'25.790"N 7°37'54.752"E	208876	502700, 502600
77	Oberer Märetschisee	VS	2360	46°15'19.194"N 7°39'01.867"E	42441	502700, 502600
78	Unterer Märetschisee	VS	2305	46°15'28.413"N 7°39'15.922"E	43309	502700, 502600
79	[Zermiggern unnamed]	VS	1738	46°04'57.470"N 7°57'26.917"E	14630	501500, 501600
80	[Oberems (Argessa) unnamed]	VS	1370	46°16'58.001"N 7°41'23.306"E	3465	502600
81	[Châtelard-Barberine unnamed]	VS	1115	46°03'40.544"N 6°57'33.964"E	17142	506700
82	[Peccia (Sambuco) unnamed]	TI	1032	46°24'50.832"N 8°36'37.300"E	17408	602400

* Data for associated hydro installations can be found in (Bundesamt für Energie BFE, 2018b).

A3 Exchange Rates

1 EUR = 1.09 CHF

1 USD = 0.99 CHF

1 BRL = 0.26 CHF

Source: OANDA Currency Converter (OANDA, 2019) – retrieved on August 3rd, 2019.

A4 Tables of Results by Scenario

Note: Full tables are available at <https://github.com/bonesbb/HASPR>.

Scenario 1: 100% surface area coverage, 15% efficiency

Panel Configuration	Yearly Output (TWh)	Summer Output (TWh)	Winter Output (TWh)
Case 1: Flat panels	8.8	6.2	2.6
Case 2: Tracking panels	12.0	8.1	3.9
Case 3: Fixed panels with 12-degree tilt, optimized for total production	9.3	6.4	2.9
Case 4: Fixed panels with 12-degree tilt, optimized for winter production	9.3	6.4	2.9
Case 5: Fixed panels with tilt between 30 and 65 degrees, optimized for winter production	9.5	6.2	3.3

Panel Configuration	Yearly Output - Lower Bound (TWh)	Summer Output - Lower Bound (TWh)	Winter Output - Lower Bound (TWh)
Case 1: Flat panels	1.54	1.19	0.35
Case 2: Tracking panels	0.75	0.67	0.09
Case 3: Fixed panels with 12-degree tilt, optimized for total production	1.36	1.10	0.26
Case 4: Fixed panels with 12-degree tilt, optimized for winter production	1.35	1.10	0.26
Case 5: Fixed panels with tilt between 30 and 65 degrees, optimized for winter production	1.06	0.91	0.16

Panel Configuration	Supply/Demand Mismatch Offset - Yearly (TWh)	Supply/Demand Mismatch Offset - Summer (GWh)	Supply/Demand Mismatch Offset - Winter (GWh)
Case 1: Flat panels	1.68	0.53	1.14
Case 2: Tracking panels	2.26	0.67	1.59
Case 3: Fixed panels with 12-degree tilt, optimized for total production	1.80	0.56	1.24
Case 4: Fixed panels with 12-degree tilt, optimized for winter production	1.80	0.56	1.24
Case 5: Fixed panels with tilt between 30 and 65 degrees, optimized for winter production	1.97	0.58	1.39

Panel Configuration	CO2-eq Offset - Yearly (megatons)	CO2-eq Offset - Summer (megatons)	CO2-eq Offset - Winter (megatons)
Case 1: Flat panels	717	445	272
Case 2: Tracking panels	1029	605	424
Case 3: Fixed panels with 12-degree tilt, optimized for total production	776	470	306
Case 4: Fixed panels with 12-degree tilt, optimized for winter production	776	470	306
Case 5: Fixed panels with tilt between 30 and 65 degrees, optimized for winter production	824	468	356

Panel Configuration	Expected Yearly Bid Revenue (million CHF)	Total Unsold Power due to Bid Increment (GWh)	Expected Yearly Potential Revenue (million CHF)
Case 1: Flat panels	387	18.0	388
Case 2: Tracking panels	551	18.1	551
Case 3: Fixed panels with 12-degree tilt, optimized for total production	417	18.0	418
Case 4: Fixed panels with 12-degree tilt, optimized for winter production	417	18.1	418
Case 5: Fixed panels with tilt between 30 and 65 degrees, optimized for winter production	438	18.1	439

Panel Configuration	Total Capital Costs (billion CHF)	Expected Lifetime Potential Revenue with no discount (billion CHF)	Lifetime Costs with no discount (billion CHF)
Case 1: Flat panels	10.7	9.1	16.1
Case 2: Tracking panels	N/A	12.9	N/A
Case 3: Fixed panels with 12-degree tilt, optimized for total production	12.4	9.8	18.6
Case 4: Fixed panels with 12-degree tilt, optimized for winter production	12.4	9.8	18.6
Case 5: Fixed panels with tilt between 30 and 65 degrees, optimized for winter production	N/A	10.3	N/A

Panel Configuration	Sum of NPV for Potential Revenue at 7% Discount (billion CHF)	Sum of NPV for Potential Revenue at 8% Discount (billion CHF)	Sum of NPV for Potential Revenue at 10% Discount (billion CHF)
Case 1: Flat panels	-8.74	-8.92	-9.22
Case 2: Tracking panels	-8.97 *	-9.28 *	-9.78 *
Case 3: Fixed panels with 12-degree tilt, optimized for total production	-10.45	-10.64	-10.93
Case 4: Fixed panels with 12-degree tilt, optimized for winter production	-10.46	-10.64	-10.94
Case 5: Fixed panels with tilt between 30 and 65 degrees, optimized for winter production	-10.23 *	-10.43 *	-10.75 *

* Hypothetical values assuming the same costs as 12-degree panels.

Scenario 2: 10% surface area coverage, 15% efficiency

Panel Configuration	Yearly Output (GWh)	Summer Output (GWh)	Winter Output (GWh)
Case 1: Flat panels	878	617	261
Case 2: Tracking panels	1201	807	394
Case 3: Fixed panels with 12-degree tilt, optimized for total production	934	644	290
Case 4: Fixed panels with 12-degree tilt, optimized for winter production	933	643	290
Case 5: Fixed panels with tilt between 30 and 65 degrees, optimized for winter production	952	620	332

Panel Configuration	Yearly Output - Lower Bound (GWh)	Summer Output - Lower Bound (GWh)	Winter Output - Lower Bound (GWh)
Case 1: Flat panels	154	119	35
Case 2: Tracking panels	75	67	9
Case 3: Fixed panels with 12-degree tilt, optimized for total production	136	110	26
Case 4: Fixed panels with 12-degree tilt, optimized for winter production	135	110	26
Case 5: Fixed panels with tilt between 30 and 65 degrees, optimized for winter production	106	91	16

Panel Configuration	Supply/Demand Mismatch Offset - Yearly (GWh)	Supply/Demand Mismatch Offset - Summer (GWh)	Supply/Demand Mismatch Offset - Winter (GWh)
Case 1: Flat panels	271	109	162
Case 2: Tracking panels	415	160	254
Case 3: Fixed panels with 12-degree tilt, optimized for total production	300	118	182
Case 4: Fixed panels with 12-degree tilt, optimized for winter production	301	119	183
Case 5: Fixed panels with tilt between 30 and 65 degrees, optimized for winter production	341	127	213

Panel Configuration	CO2-eq Offset - Yearly (megatonnes)	CO2-eq Offset - Summer (megatonnes)	CO2-eq Offset - Winter (megatonnes)
Case 1: Flat panels	72	44	27
Case 2: Tracking panels	103	60	42
Case 3: Fixed panels with 12-degree tilt, optimized for total production	78	47	31
Case 4: Fixed panels with 12-degree tilt, optimized for winter production	78	47	31
Case 5: Fixed panels with tilt between 30 and 65 degrees, optimized for winter production	82	47	36

Panel Configuration	Expected Yearly Bid Revenue (million CHF)	Total Unsold Power due to Bid Increment (GWh)	Expected Yearly Potential Revenue (million CHF)
Case 1: Flat panels	38.0	17.1	38.8
Case 2: Tracking panels	54.3	17.7	55.1
Case 3: Fixed panels with 12-degree tilt, optimized for total production	41.0	17.2	41.8
Case 4: Fixed panels with 12-degree tilt, optimized for winter production	41.0	17.2	41.8
Case 5: Fixed panels with tilt between 30 and 65 degrees, optimized for winter production	43.0	17.2	43.9

Panel Configuration	Total Capital Costs (billion CHF)	Expected Lifetime Potential Revenue with no discount (billion CHF)	Lifetime Costs with no discount (billion CHF)
Case 1: Flat panels	1.07	0.91	1.61
Case 2: Tracking panels	N/A	1.29	N/A
Case 3: Fixed panels with 12-degree tilt, optimized for total production	1.24	0.98	1.86
Case 4: Fixed panels with 12-degree tilt, optimized for winter production	1.24	0.98	1.86
Case 5: Fixed panels with tilt between 30 and 65 degrees, optimized for winter production	N/A	1.03	N/A

Panel Configuration	Sum of NPV for Potential Revenue at 7% Discount (million CHF)	Sum of NPV for Potential Revenue at 8% Discount (million CHF)	Sum of NPV for Potential Revenue at 10% Discount (million CHF)
Case 1: Flat panels	-874	-892	-922
Case 2: Tracking panels	-897 *	-928 *	-977 *
Case 3: Fixed panels with 12-degree tilt, optimized for total production	-1045	-1064	-1093
Case 4: Fixed panels with 12-degree tilt, optimized for winter production	-1046	-1064	-1094
Case 5: Fixed panels with tilt between 30 and 65 degrees, optimized for winter production	-1023 *	-1043 *	-1075 *

* Hypothetical values assuming the same costs as 12-degree panels.

Scenario 3: 1% surface area coverage, 15% efficiency

Panel Configuration	Yearly Output (GWh)	Summer Output (GWh)	Winter Output (GWh)
Case 1: Flat panels	87.8	61.7	26.1
Case 2: Tracking panels	120.1	80.7	39.4
Case 3: Fixed panels with 12-degree tilt, optimized for total production	93.4	64.4	29.0
Case 4: Fixed panels with 12-degree tilt, optimized for winter production	93.3	64.3	29.0
Case 5: Fixed panels with tilt between 30 and 65 degrees, optimized for winter production	95.2	62.0	33.2

Panel Configuration	Yearly Output - Lower Bound (GWh)	Summer Output - Lower Bound (GWh)	Winter Output - Lower Bound (GWh)
Case 1: Flat panels	15.4	11.9	3.5
Case 2: Tracking panels	7.5	6.7	0.9
Case 3: Fixed panels with 12-degree tilt, optimized for total production	13.6	11.0	2.6
Case 4: Fixed panels with 12-degree tilt, optimized for winter production	13.5	11.0	2.6
Case 5: Fixed panels with tilt between 30 and 65 degrees, optimized for winter production	10.6	9.1	1.6

Panel Configuration	Supply/Demand Mismatch Offset - Yearly (GWh)	Supply/Demand Mismatch Offset - Summer (GWh)	Supply/Demand Mismatch Offset - Winter (GWh)
Case 1: Flat panels	28.5	11.7	16.8
Case 2: Tracking panels	43.8	17.4	26.4
Case 3: Fixed panels with 12-degree tilt, optimized for total production	31.6	12.7	18.9
Case 4: Fixed panels with 12-degree tilt, optimized for winter production	31.7	12.7	18.9
Case 5: Fixed panels with tilt between 30 and 65 degrees, optimized for winter production	35.8	13.7	22.1

Panel Configuration	CO2-eq Offset - Yearly (megatons)	CO2-eq Offset - Summer (megatons)	CO2-eq Offset - Winter (megatons)
Case 1: Flat panels	7.2	4.4	2.7
Case 2: Tracking panels	10.3	6.0	4.2
Case 3: Fixed panels with 12-degree tilt, optimized for total production	7.8	4.7	3.1
Case 4: Fixed panels with 12-degree tilt, optimized for winter production	7.8	4.7	3.1
Case 5: Fixed panels with tilt between 30 and 65 degrees, optimized for winter production	8.2	4.7	3.6

Panel Configuration	Expected Yearly Bid Revenue (million CHF)	Total Unsold Power due to Bid Increment (GWh)	Expected Yearly Potential Revenue (million CHF)
Case 1: Flat panels	3.3	12.7	3.9
Case 2: Tracking panels	4.8	14.0	5.5
Case 3: Fixed panels with 12-degree tilt, optimized for total production	3.6	12.9	4.2
Case 4: Fixed panels with 12-degree tilt, optimized for winter production	3.6	12.9	4.2
Case 5: Fixed panels with tilt between 30 and 65 degrees, optimized for winter production	3.8	12.9	4.4

Panel Configuration	Total Capital Costs (billion CHF)	Expected Lifetime Potential Revenue with no discount (billion CHF)	Lifetime Costs with no discount (billion CHF)
Case 1: Flat panels	0.11	0.09	0.16
Case 2: Tracking panels	N/A	0.13	N/A
Case 3: Fixed panels with 12-degree tilt, optimized for total production	0.12	0.10	0.19
Case 4: Fixed panels with 12-degree tilt, optimized for winter production	0.12	0.10	0.19
Case 5: Fixed panels with tilt between 30 and 65 degrees, optimized for winter production	N/A	0.10	N/A

Panel Configuration	Sum of NPV for Potential Revenue at 7% Discount (million CHF)	Sum of NPV for Potential Revenue at 8% Discount (million CHF)	Sum of NPV for Potential Revenue at 10% Discount (million CHF)
Case 1: Flat panels	-87.4	-89.2	-92.2
Case 2: Tracking panels	-89.7 *	-92.8 *	-97.7 *
Case 3: Fixed panels with 12-degree tilt, optimized for total production	-104.5	-106.4	-109.3
Case 4: Fixed panels with 12-degree tilt, optimized for winter production	-104.6	-106.4	-109.4
Case 5: Fixed panels with tilt between 30 and 65 degrees, optimized for winter production	-102.3 *	-104.3 *	-107.5 *

* Hypothetical values assuming the same costs as 12-degree panels.

LCOE Results: (independent of scenarios)

Panel Configuration	Average LCOE - 7% Discount (CHF cents/kWh)	Average LCOE - 8% Discount (CHF cents/kWh)	Average LCOE - 10% Discount (CHF cents/kWh)
Case 1: Flat panels	0.74	1.74	3.82
Case 2: Tracking panels	0.62 *	1.47 *	3.22 *
Case 3: Fixed panels with 12-degree tilt, optimized for total production	0.80	1.89	4.15
Case 4: Fixed panels with 12-degree tilt, optimized for winter production	0.80	1.89	4.15
Case 5: Fixed panels with tilt between 30 and 65 degrees, optimized for winter production	0.79 *	1.85 *	4.07 *

* Hypothetical values assuming the same costs as 12-degree panels.

References

- Abrell, J. (2017). The Swiss Wholesale Electricity Market. *ETH Zürich* [Online]. Retrieved from: https://ethz.ch/content/dam/ethz/special-interest/mtec/cer-eth/economics-energy-economics-dam/documents/people/jabrell/Abrell_Swiss_Wholesale_Electricity_Market.pdf [Accessed 2019].
- Andenæs, E., Jelle, B. P., Ramlø, K., Kolås, T., Selj, J., & Foss, S. E. (2018). The influence of snow and ice coverage on the energy generation from photovoltaic solar cells. *Solar Energy*, 159, pp. 318-328.
- Antonanzas, J., Osorio, N., Escobar, R., Urraca, R., Martinez-de-Pison, F. J., & Antonanzas-Torres, F. (2016). Review of photovoltaic power forecasting. *Solar Energy*, 136, pp. 78-111.
- Awad, H., Güll, M., Salim, K. M. E., & Yu, H. (2018). Predicting the energy production by solar photovoltaic systems in cold-climate regions. *International Journal of Sustainable Energy*, 37(10), pp. 978-998.
- Bartlett, S., Dujardin, J., Kahl, A., Kruyt, B., Manso, P., & Lehning, M. (2018). Charting the course: A possible route to a fully renewable Swiss power system. *Energy*, 163, pp. 942-955.
- Beniston, M. (2012). Impacts of climatic change on water and associated economic activities in the Swiss Alps. *Journal of Hydrology*, 412, pp. 291-296.
- Blumthaler, M. (2012). Solar radiation of the high alps. In *Plants in Alpine Regions* (pp. 11-20). Springer, Vienna.
- Bundesamt für Energie BFE. (2018a). Energiestrategie 2050 - Monitoring Bericht 2018 - Langfassung. *Bundesamt für Energie* [Online]. Retrieved from: https://www.bfe.admin.ch/bfe/de/home/versorgung/statistik-und-geodaten/monitoring-energiestrategie-2050/_jcr_content/par/tabs/items/tab/tabpar/externalcontent.external.exturl.pdf/aHR0cHM6Ly9wdWJkYi5iZmUuYWRtaW4uY2gvZGUvcHVibGljYX/Rpb24vZG93bmrvYWQvOTUyMy5wZGY=.pdf [Accessed 2019].
- Bundesamt für Energie BFE. (2018b). Statistik der Wasserkraftanlagen der Schweiz. *Bundesamt für Energie* [Online]. Retrieved from: https://www.bfe.admin.ch/bfe/de/home/versorgung/statistik-und-geodaten/energiestatistiken/teilstatistiken/_jcr_content/par/tabs/items/tab/tabpar/externalcontent.external.exturl.zip/aHR0cHM6Ly9wdWJkYi5iZmUuYWRtaW4uY2gvZGUvcHVibGljYX/Rpb24vZG93bmrvYWQvOTMzOS56aXA=.zip [Accessed 2019].
- Bundesamt für Energie BFE. (2019). Schweizerische Elektrizitätsstatistik 2018. *Bundesamt für Energie* [Online]. Retrieved from: https://www.bfe.admin.ch/bfe/en/home/supply/statistics-and-geodata/energy-statistics/electricity-statistics/_jcr_content/par/tabs/items/tab/tabpar/externalcontent.external.exturl.pdf/aHR0cHM6Ly9wdWJkYi5iZmUuYWRtaW4uY2gvZGUvcHVibGljYX/Rpb24vZG93bmrvYWQvOTc0OC5wZGY=.pdf [Accessed 2019].
- Campana, P. E., Wästhage, L., Nookuea, W., Tan, Y., & Yan, J. (2019). Optimization and assessment of floating and floating-tracking PV systems integrated in on- and off-grid hybrid energy systems. *Solar Energy*, 177, pp. 782-795.
- Cazzaniga, R., Cicu, M., Rosa-Clot, M., Rosa-Clot, P., Tina, G. M., & Ventura, C. (2018). Floating photovoltaic plants: Performance analysis and design solutions. *Renewable and Sustainable Energy Reviews*, 81, pp. 1730-1741.
- Cazzaniga, R., Rosa-Clot, M., Rosa-Clot, P., & Tina, G. M. (2019). Integration of PV floating with hydroelectric power plants. *Heliyon*, 5(6), p. e01918.
- Charles Lawrence Kamuyu, W., Lim, J., Won, C., & Ahn, H. (2018). Prediction model of photovoltaic module temperature for power performance of floating PVs. *Energies*, 11(2), p. 447.
- Chevrier, A., Smith, R., & Bollinger, A. (2016). Calculation of a dynamic carbon factor for the Swiss electricity grid. *ETH Zürich / EMPA* [Online]. Retrieved from: https://hues.empa.ch/images/Alice_Chevrier_Semester_Project.pdf [Accessed 2019].

- Chitturi, S. R. P., Sharma, E., & Elmenreich, W. (2018). Efficiency of photovoltaic systems in mountainous areas. In *2018 IEEE International Energy Conference (ENERGYCON)*, pp. 1-6. IEEE.
- Ciel & Terre International. (2019). Hydrello: The Patented Floating PV System. *Ciel & Terre International* [Online]. Retrieved from: <https://www.ciel-et-terre.net/hydrello-floating-solar-technology/hydrello-products/> [Accessed 2019].
- CleanTechnica. (2019). What's Not To Love About Floating Solar Farms. *CleanTechnica* [Online]. Retrieved from: <https://cleantechnica.com/2019/05/13/whats-not-to-love-about-floating-solar-farms-cleantechnica-interview/> [Accessed 2019].
- Darling, S. B., You, F., Veselka, T., & Velosa, A. (2011). Assumptions and the levelized cost of energy for photovoltaics. *Energy & Environmental Science*, 4(9), pp. 3133-3139.
- Davis, S. J., Lewis, N. S., Shaner, M., Aggarwal, S., Arent, D., Azevedo, I. L., Benson, S. M., Bradley, T., Brouwer, J., Chiang, Y. M., & Clack, C. T. (2018). Net-zero emissions energy systems. *Science*, 360(6396), p. eaas9793.
- Díaz, P., & Van Vliet, O. (2018). Drivers and risks for renewable energy developments in mountain regions: a case of a pilot photovoltaic project in the Swiss Alps. *Energy, Sustainability and Society*, 8(1), p. 28.
- Durisch, W., & Bulgheroni, W. (1999). Climatological investigation for solar-power stations in the Swiss Alps. *Applied energy*, 64(1-4), pp. 411-415.
- ENTSO-E Transparency Platform. (2019). Day-ahead Prices - Switzerland. *ENTSO-E* [Online]. Retrieved from: <https://transparency.entsoe.eu> [Accessed 2019].
- Er, Z., Rouabah, Z., Kizilkan, G., & Orken, A. T. (2018). Standards and testing experiments for a photovoltaic module. *Avrupa Bilim ve Teknoloji Dergisi*, (Özel Sayı-Special Issue), pp. 12-15.
- Federal Office of Topography swisstopo. (2019). Interactive Map of Official Survey and Geological Data Sets. *Federal Office of Topography swisstopo* [Online]. Retrieved from: <https://map.geo.admin.ch/> [Accessed 2019].
- Hansen, J., Sato, M., Hearty, P., Ruedy, R., Kelley, M., Masson-Delmotte, V., Russell, G., Tselioudis, G., Cao, J., Rignot, E., & Velicogna, I. (2016). Ice melt, sea level rise and superstorms: evidence from paleoclimate data, climate modeling, and modern observations that 2 C global warming could be dangerous. *Atmospheric Chemistry and Physics*, 16(6), pp. 3761-3812.
- Hay, J. E. (1993). Calculating solar radiation for inclined surfaces: Practical approaches. *Renewable Energy*, 3(4), pp. 373-380.
- Kahl, A., Dujardin, J., & Lehning, M. (2019). The bright side of PV production in snow-covered mountains. *Proceedings of the National Academy of Sciences*, 116(4), pp. 1162-1167.
- Karlsson, K.-G., Anttila, K., Trentmann, J., Stengel, M., Meirink, J. F., Devasthale, A., Hanschmann, T., Kothe, S., Jääskeläinen, E., Sedler, J., Benas, N., van Zadelhoff, G.-J., Schlundt, C., Stein, D., Finkensieper, S., Håkansson, N., Hollmann, R., Fuchs, P., & Werscheck, M. (2017). CLARA-A2: CM SAF Cloud, Albedo and Surface Radiation dataset from AVHRR data - Edition 2. *Satellite Application Facility on Climate Monitoring* [Online]. Retrieved from: https://doi.org/10.5676/EUM_SAF_CM/CLARA_AVHRR/V002 [Accessed 2019].
- Khiareddine, A., Ben Salah, C., Rekioua, D., & Mimouni, M. F. (2018). Sizing methodology for hybrid photovoltaic/wind/hydrogen/battery integrated to energy management strategy for pumping system. *Energy*, 153, pp. 743-762.
- Lave, M., Hayes, W., Pohl, A., & Hansen, C. W. (2015). Evaluation of global horizontal irradiance to plane-of-array irradiance models at locations across the United States. *IEEE journal of Photovoltaics*, 5(2), pp. 597-606.
- OANDA. (2019). OANDA Currency Converter. *OANDA* [Online]. Retrieved from: <https://www1.oanda.com/currency/converter/> [Accessed August 3rd, 2019].
- Pfeifroth, U., Kothe, S., Trentmann, J., Hollmann, R., Fuchs, P., Kaiser, J., & Werscheck, M. (2019). Surface Radiation Data Set - Heliosat (SARAH) - Edition 2.1. *Satellite Application Facility on Climate Monitoring* [Online]. Retrieved from: https://doi.org/10.5676/EUM_SAF_CM/SARAH/V002_01 [Accessed 2019].
- Pysolar Development Team. (2019). Pysolar Python library. *Pysolar* [Online]. Retrieved from: <http://docs.pysolar.org/en/latest/> [Accessed 2019].

- Ranjbaran, P., Yousefi, H., Gharehpetian, G. B., & Astaraei, F. R. (2019). A review on floating photovoltaic (FPV) power generation units. *Renewable and Sustainable Energy Reviews*, 110, pp. 332-347.
- Silvério, N. M., Barros, R. M., Tiago Filho, G. L., Redón-Santafé, M., Santos, I. F. S. d., & Valério, V. E. d. M. (2018). Use of floating PV plants for coordinated operation with hydropower plants: Case study of the hydroelectric plants of the São Francisco River basin. *Energy Conversion and Management*, 171, pp. 339-349.
- Swissgrid. (2019). Energy Statistic Switzerland 2018. *Swissgrid* [Online]. Retrieved from: <https://www.swissgrid.ch/dam/dataimport/energy-statistic/EnergieUebersichtCH-2018.xls> [Accessed 2019].
- U.S. Energy Information Administration. (2019). CO2 Emissions from Coal - Europe. *U.S. Energy Information Administration* [Online]. Retrieved from: https://www.eia.gov/beta/international/data/browser/#/?pa=00000000000000000000000000000000g&c=0000000000000002&tl_id=1-A&vs=INTL.1-8-EURO-MMTCD.A&ord=CR&vo=0&v=T&start=1980&end=2016&s=INTL.1-8-EURO-MMTCD.A [Accessed 2019].
- World Bank Group, ESMAP, & SERIS. (2018). Where Sun Meets Water: Floating Solar Market Report - Executive Summary. *Washington, DC: World Bank* [Online]. Retrieved from: <http://documents.worldbank.org/curated/en/579941540407455831/pdf/Floating-Solar-Market-Report-Executive-Summary.pdf> [Accessed 2019].